

# Turbidite-Hosted Gold Mineralization at the Dolaucothi Gold Mines, Dyfed, Wales, United Kingdom

A. E. ANNELS

*Department of Geology, University of Wales, College of Cardiff, Cardiff CF1 3yE, Wales*

AND D. E. ROBERTS

*Department of Geology, University of Bristol, Bristol BS8 1TH, United Kingdom*

## Abstract

The Dolaucothi gold deposit occurs in thin bedded turbidites of Upper Ordovician to basal Silurian age deposited near the southern margin of the lower Paleozoic Welsh basin. The host rocks were deformed during the Caledonian orogeny (390–410 Ma) into a series of inclined asymmetrical, commonly overturned, tight southeast-facing folds with associated cleavage. Reverse dip-slip faults accompanied the folding and the whole area is cut by late tensional faults. The mineralization is controlled by structures produced during the Caledonian orogeny, in particular a thrust fault which formed the host to the Roman lode, a flat-lying auriferous quartz reef up to 6 m thick.

Gold occurs in a variety of hosts including pyritic shales containing both euhedral and framboidal pyrite, quartz-carbonate stringer veins, in steeply or gently inclined veins associated with shear zones and in planar quartz veins associated with the Roman lode. The mineralogy is simple, with pyrite and arsenopyrite being the dominant sulfides. Ankeritic carbonates, hydromuscovite, and the lithium silicate, cookeite, are also present.

It is proposed that, during prograde metamorphism associated with early stages of the Caledonide orogeny, fluids circulated through the basement below the southeast margin of the Welsh basin and leached gold, and associated metals, from rocks of igneous or volcanic origin. These overpressured fluids were released to high crustal levels during later orogenic movements and uplifts, perhaps related to reactivation of such basement faults as the infra-Tywi fault. Geothermometric studies indicate that the host rocks experienced upper anchizone facies metamorphism whereas the temperatures of the mineralizing fluids were in the range of 345° to 450°C. Isotopic studies point to a common origin for the sulfides in both the shales and the veins and also indicate that the host rocks provided the source of the carbon now incorporated in the carbonates.

## Introduction

THOUGH the gold veins of the Dolgellau area (Fig. 1) are relatively well known because they provided the gold for wedding rings for the British Royal Family, those at Dolaucothi are less familiar to the populace at large and also to geologists interested in gold mineralization. They are situated about 1 km southeast of the village of Pumsaint, between Lampeter and Llandovery in the county of Dyfed, Wales (Fig. 2). The main workings can be traced for a distance of approximately 1.1 km along the northwestern flanks of a mountain spur separating the Cothi and Annell River valleys (Fig. 3). The orientation of this spur follows the local trend of Caledonide folding. The mine workings have a complex history and comprise a series of open pits, trenches, adits, and shafts which range in age from Roman (AD 75–150) to 20th century (1935–1939). Most of the more recent workings are concentrated around the Ogofau pit, a large excavation of Roman origin. Though the Dolaucothi area is dominated by gold mineralization, the surrounding

areas contain only lead-zinc-bearing quartz veins devoid of gold.

Genetic theories for the origin of gold veins hosted by turbidites distant from any volcanic or associated igneous activity require an explanation for the source of the gold, the nature of the transporting hydrothermal fluids, and the factors controlling the localization of the mineralization. Recent papers in Keppie et al. (1986) have addressed this problem and have shown that these deposits can be categorized as a distinct group clearly related to prograde metamorphism and tectonism associated with an orogenic event.

This paper describes for the first time the nature of the gold occurrence at the Dolaucothi mines. Interpretations of the results of research here have implications for the understanding of the genesis of gold deposits in turbidites in general.

## Sources of Information

Very little published information exists on the mine. The available records are concerned dominantly with

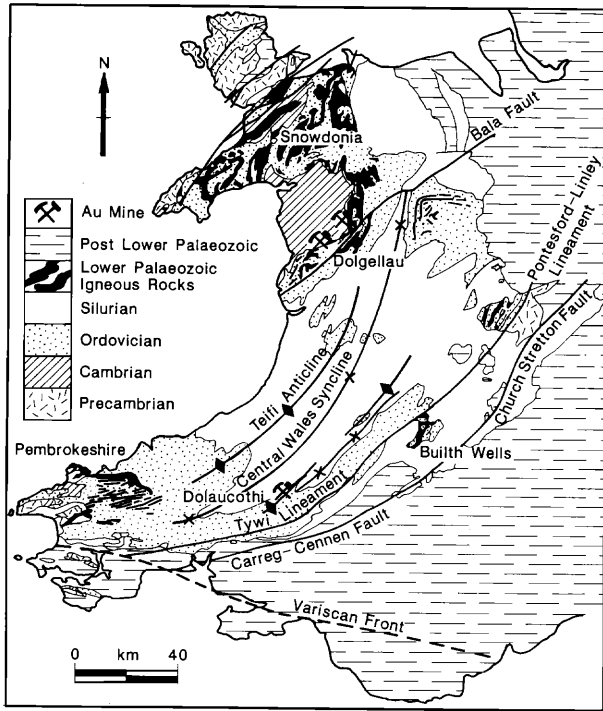


FIG. 1. Simplified geologic map of Wales and the Welsh Borderland showing the main structural elements and localities referred to in the text.

the mining and processing of the gold ores (Holman, 1911; Nelson, 1944; Hall, 1971). Reliable geologic information is scarce, but unpublished consultancy reports, together with mine captains' reports for a

limited period toward the end of the mine's life, do throw some light on the nature of the auriferous lodes and the geology of the mine itself. Some detailed mineralogical information on cookeite and hydromuscovite (illite) at Ogofau is also available (Brammall et al., 1937; Nagelschmidt, 1937). A review of the mining history of the site, from Roman times to 1939, appears in Annel and Burnham (1986) together with a preliminary geologic interpretation.

Although surface and underground exposures are available for study at the mine, these are dominantly in the footwall of the Roman lode, a flat-lying quartz reef exploited by both the Romans and later miners. Though very useful in developing theories of ore genesis and in elucidating the structural environment of the gold deposits, these exposures do not give much information on the exact nature of this lode in particular and its mode of emplacement. All accessible adits have been carefully mapped by the authors at a scale of 1:100 and sampled for mineralogical and assay purposes. The main shaft (New shaft) which was initially sunk in 1909 and then deepened over the period 1933 to 1938, is flooded and blocked with debris and thus is no longer accessible. However, mine plans dated 1935 and 1939, together with assay plans dated 1910 and 1938, do give some indication as to the configuration of the Roman lode especially when combined with diagrams appearing in Nelson (1944). Additional information has been gained from six holes drilled in the Ogofau pit by University College, Cardiff, since 1985 and from the results of drilling on Allt y Brunant, 1 km to the northeast of Ogofau, undertaken by Anglo-Canadian Exploration (ACE), Ltd.,

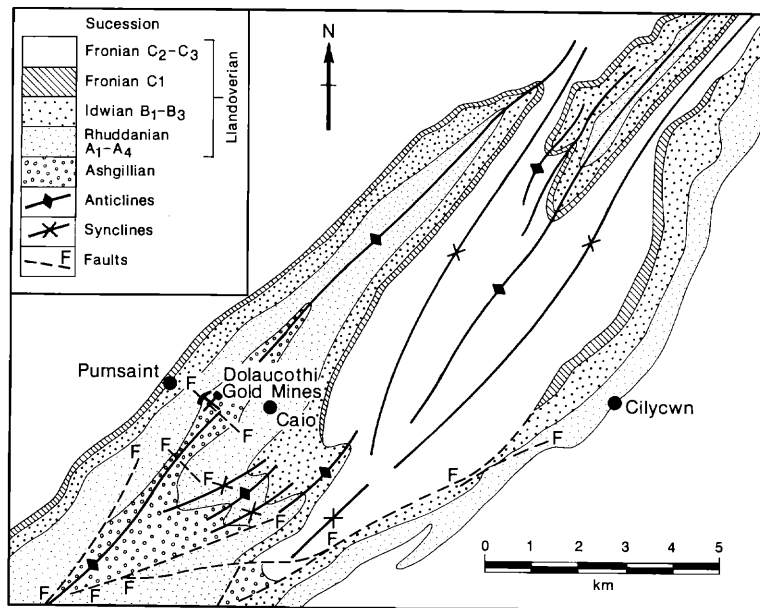


FIG. 2. Geologic map of the Cothi anticline showing the location of the Dolaucothi gold mines.

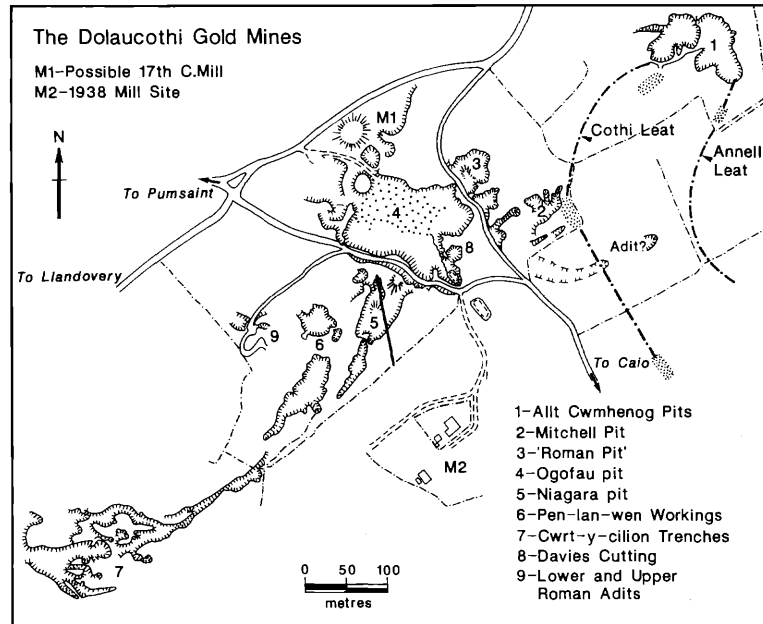


FIG. 3. Surface workings associated with the Dolaucothi lode zone together with the location of the main adits.

of Toronto, Canada, in 1980. Two Master of Science theses have also been written on aspects of the primary and secondary geochemistry of the Dolaucothi area. One of these studies (Tater, 1975) provides useful lithogeochemical data on the alteration associated with the gold mineralization.

### Regional Geology

During the lower Paleozoic, the area which is now Wales formed part of the southern continental margin of the Iapetus ocean (Phillips et al., 1976; Dewey, 1982; Kokelaar et al., 1984). A structurally controlled ensialic marginal basin, the Welsh basin (approx. 200 by 100 km in size) accumulated a thick (up to 15 km) sequence of shallow- and deep-water sediments while, to the south and east, a relatively stable platform accumulated a thinner (5 km) sequence of shallow-water sediments. The southern margin of the Welsh basin lies virtually along the line of the Pontesford-Linley fault (Fig. 1) and its projected continuation southward into the Tywi lineament. Thick sediments were accumulated in this basin during Cambrian times, but during the Lower Ordovician, localized volcanic activity accompanied sedimentation. This activity reached its peak during the Caradocian and had virtually ceased by Early Silurian times.

During the Upper Ordovician and the Llandoverian, sedimentation in the Welsh basin was greatly influenced by intrabasinal and basin-margin faults (James and James, 1969). These faults triggered slump and turbidity currents which resulted in the progra-

vation of small submarine fans both parallel to the basin margins and across the basin itself. James and James (1969) also postulated the presence of an infra-Tywi-Severn fault at the basin margin during Late Ordovician to Early Silurian times, indicating that there was a basinward shift in the structural margin at this time.

During the lower and middle Llandoverian, there was a plentiful supply of sediment into the basin from the landmass to the south and east. Submarine fans, bird's foot deltas, and submarine channels, together with mass flow by turbidity currents, gave rise to a great thickness of graywackes and other turbidite facies sediments. During the upper Llandoverian, there was a major marine transgression on to the platform, and during the succeeding Wenlock and Ludlow times, it is likely that the structural margin of the basin moved southeast to the line of the Church Stretton fault. Throughout its long history, the southern margin of the Welsh basin appears to have fluctuated in position between definite and clearcut structural lineaments.

The host rocks to the gold mineralization at Dolaucothi are Upper Ordovician (probably uppermost Ashgillian but no older than the *Dicellograptus clinigani* zone), and they are overlain by a complete Llandoverian sequence from the *Glyptograptus presculpatus* to the *Monograptus crenulatus* zone.

Absolute dating of the various subdivisions of the Ordovician and Silurian of central Wales has been a controversial matter; the results given by the main protagonists are shown in Table 1. These dates indi-

TABLE 1. Stratigraphic Succession of Central Wales

Stratigraphy	Age ranges	
	McKerrow et al. (1980)	Gale et al. (1980)
	(Ma)	(Ma)
Devonian	360–411	360–400
Pridoli	411–413.5	
Silurian		400–425
Ludlow	413.5–420	
Wenlock	420–425.5	
Ordovician		425–500
Llandovery	425.5–438	} Mine sequence
Ashgill	438–445	
Caradoc	445–467	
Llandeilo	467–479	
Llanvirn	478–489	
Arenig	489–504	
Tremadoc	504–519	

Caledonide orogeny 390–410 Ma

cate a time span of 75 to 81 Ma for the Ordovician and 25 to 27 Ma for the Silurian. The main phase of the Caledonian orogeny in South Wales was a mid-Devonian event (374–387 Ma), the Lower Devonian having undergone the same pattern of deformation as the underlying Silurian. The Upper Devonian clearly lies on an angular unconformity.

During the Caledonian orogeny the lower Paleozoic rocks of Wales were folded into a number of large-scale, mainly northeast-southwest structures (Fig. 1) with associated subsidiary folds. However, this trend changes to a more westerly direction in the southwest, reflecting the position and orientation of the basin margin. The folding was accompanied by a period of cleavage development approximately axial parallel to the folds. This cleavage is distinct throughout most of central Wales, although it is best developed in the famous Cambrian slate belt of Gwynedd (northwest Wales) and is well displayed in the more pelitic sediments at the Dolaucothi mines. After the folding, a number of major faults were developed, many a reactivation of older structures, such as the Pontesford-Linley and Church Stretton faults and their continuations southwestward along the margin of the Welsh basin.

Current understanding of the structures in the southern half of Wales, from the Teifi anticline to the Church Stretton-Carreg-Cennen disturbance, still relies heavily on the detailed mapping undertaken by Jones (1912). The Teifi anticline is essentially a broad northeasterly trending anticline with numerous asymmetrical parasitic folds on its limbs. The central Wales syncline separates this anticline from the Tywi anticline to the southeast, both of which have a northeasterly trend. The Tywi anticline probably began its

development in Llandoveryian (or even Ashgillian) times. Subsidiary asymmetrical folds overturned to the southeast, together with associated high-angle reverse faults, have developed along the northwestern flanks of this major structure and are aligned parallel to its postulated axial trace. The Dolaucothi gold mineralization occurs in the central section of one such fold, the Cothi anticline (Fig. 2).

## Geology of the Mineralized Zone

### *Lithologies and sedimentology*

The host rocks to the gold mineralization are a monotonous sequence of thin bedded shales and siltstones, the product of turbidity flows. Since the area is close to the postulated southern margin of the Welsh basin, they could represent levee deposits formed closer to the basin slope. Surface and underground exposures, and also drill core, reveal that the host rocks consist of a repetitive sequence of five main lithological types, each representing a transition from rocks containing dominantly silt-grade material to black shales. The transition from silt to shale is rarely complete, and a detailed stratigraphic sequence has not yet been fully established due to structural interference and the absence of marker horizons. No rocks of volcanic origin have been recorded at the mine nor, indeed, in the whole of the Cothi anticline.

The black shales (BS) are essentially homogeneous, and only faint traces of bedding are discernible, although <1-mm-thick bands of silt are locally present. Color banding is not distinct, but a strong fissility is related to the presence of a dominant cleavage. These shales grade into, or are intercalated with, banded black shales (BBS) which show a distinct banding due to the variable silt content of the shale. They resemble the black shales, but they have a well-developed bedding plane fissility due to the abundance of 1-mm-thick silty bands. Where weathered, the color banding is pronounced. Laminated siltstone bands, between 5 and 10 mm thick, are occasionally found.

Banded black shales and siltstones (BBSS) superficially resemble the banded black shale unit since they are color banded, but they contain up to 20 percent siltstone bands, 5 to 10 mm thick. Lithological contacts are sharp and bedding in the siltstone is generally laminar; rare examples of ripple-drift bedding have been recorded. The banded black shales and siltstone unit is easily mistaken for the shale and siltstone (SS) lithology, but it has siltstone bands 10 to 20 mm thick constituting at least 40 percent of the rock, along with thinner seams. A transition zone may exist between these two units making recognition of contacts difficult in the field. The siltstone bands may have a lensoid or discontinuous nature and many display sharply defined, commonly erosional, basal con-

tacts; the upper contact is represented by a rapid transition into the overlying shale. Laminar and ripple drift bedding are both common, as is evidence of penecontemporaneous slumping and disruption of the siltstone bands. In all cases, the siltstone is uniformly fine grained, with little evidence of graded bedding.

The coarsest grained lithology is referred to as shales and quartzite (SQ) for it contains conspicuous fine-grained quartzite bands comprising as much as 60 percent of the rock. These bands range in thickness from 20 to 100 mm, and commonly show crossbedded slump structures, load casts, and other bottom structures. Lenticular bedding is common, but there is some evidence of planar bedding. The shales and quartzite lithotype has a very flaggy appearance and is the most easily recognized unit in both underground and surface exposures. Cleavage is rare.

Marker quartzites, up to 35 cm thick, consist of units of fine-grained quartzite and siltstone bands (5–10 cm thick) with only thin shale partings; rarely, such units consist entirely of quartzite. These bands have been used to clarify local structural complexities, particularly in the Roman adits (Fig. 4), but because of their restricted extent, they are of little regional use.

*Structure*

The black shale and siltstone sequence at Dolaucothi was severely deformed during the Caledonide orogeny, producing a complex pattern of folds, shear zones and faults (Figs. 4 and 5).

*Folds:* Two major styles of mesofolds exist, namely, open upright folds and inclined tight asymmetrical folds (Fig. 6). However, the former have only been

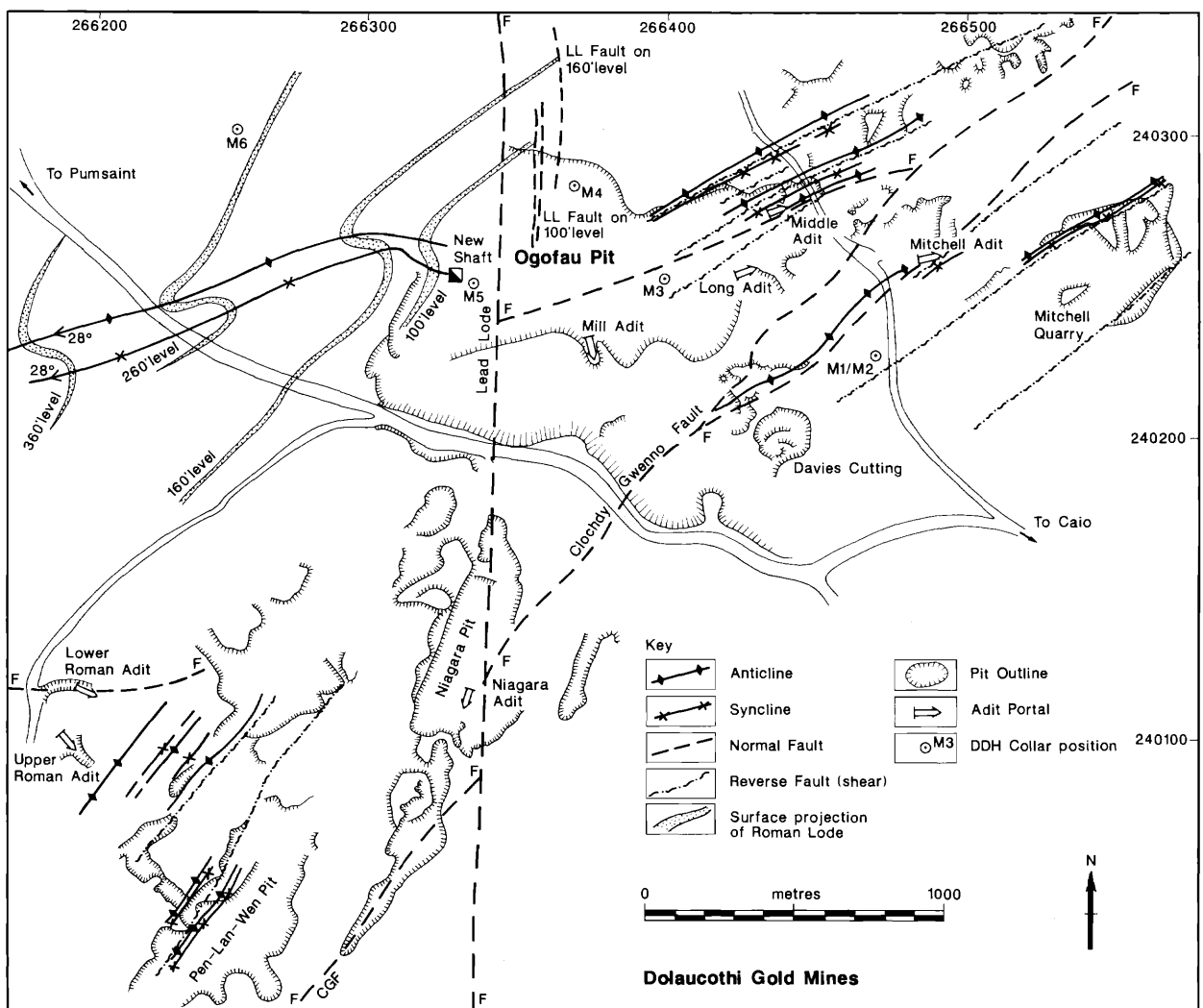


FIG. 4. Map of the central section of the Dolaucothi lode zone (the Ogofau pit) showing workings and main structural elements. LL = Lead lode.

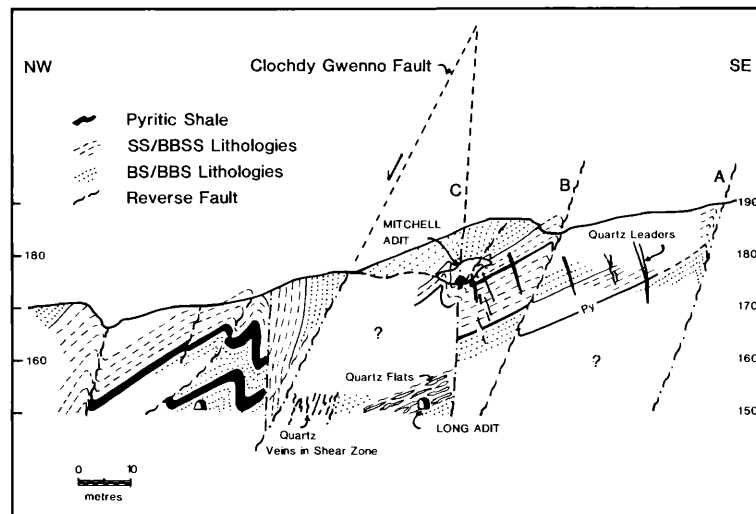


FIG. 5. Cross section to the northeast of the Ogofau pit through the Long and Mitchell adits. See Figure 11 for location of the section line.

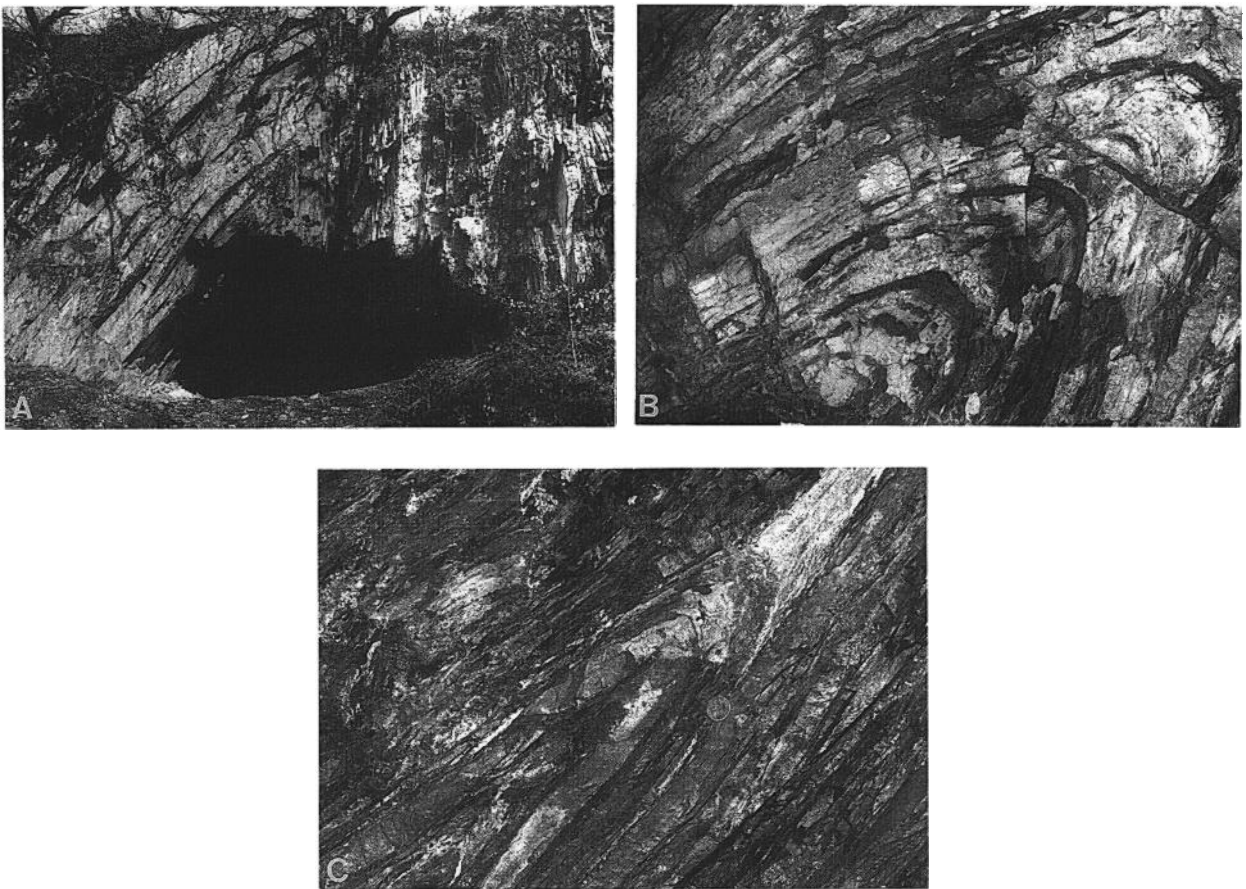


FIG. 6. Fold structures exposed around the Ogofau pit. A. Entrance to the Middle adit. B and C. Folds in pyritic shale in Davies cutting.

noted in the Roman adits (9 in Fig. 3). Minor folds are present in the hinge zones and an axial planar cleavage is ubiquitous. More common are the inclined, southeasterly verging, tight asymmetrical folds which have a longer, more gently inclined, limb and a short steeper, commonly overturned, limb. These folds form prominent structures at the entrances of both the Middle (Fig. 6a) and Mitchell adits.

Minor folds are present, though not of great significance. They include isolated open recumbent folds, indicating some late vertical shortening, and late-stage kink folds.

**Faults:** Most asymmetrical folds have steep, or gently inclined, reverse dip-slip faults associated with the overturned or steeper limb. A tentative suggestion is that the faults are listric in nature, with the folds developed as overriding structures. Tectonic transport is to the southeast, and it is proposed that the whole set of structures represents a series of imbricate thrusts, perhaps related to compaction of the sedimentary pile against the steplike structural margins of the Welsh basin. A more thorough investigation on a regional scale is required to substantiate this proposal. There is a close relationship between these thrusts and hydrothermal alteration which, in many cases, has led to pyritization of the black shales.

Late dip-slip oblique faults are also present, the most important of which is the Clochdy Gwenno fault with an average dip of  $62^\circ$  on a bearing of  $310^\circ$  (Figs. 4 and 5). The Lead Lode is another normal fault, with a dip of approximately  $85^\circ$  east, which has been located underground on the 100- and 160-ft levels, and also in drill holes. The relationship of these faults to one another cannot be observed directly, but detailed surface mapping suggests that the Clochdy Gwenno fault is cut and displaced by the Lead Lode fault. The former is well exposed in accessible underground workings (Mill and Long adits) where it is marked by a 0.3- to 0.5-m-thick fault gouge. Interpretative sections, such as Figure 5, indicate that the vertical throw on this fault may be as much as 75 m to the northwest but slickensides seen underground reveal that it also had a lateral component of movement. It clearly cuts and displaces earlier subvertical dip-slip faults (exposed in the entrances to both the Mitchell and Middle adits), which in turn are younger than the fold-associated reverse faults inclined at approximately  $70^\circ$  to the northwest. Thus, field evidence indicates four stages of faulting; the last two (represented by the Clochdy Gwenno and Lead Lode faults) postdate the emplacement of the gold-bearing quartz veins but predate base metal mineralization. The Lead Lode contains significant concentrations of argentiferous galena probably emplaced during a post-Caledonide event (343–375 Ma; Ineson and Mitchell, 1975) during which the central Wales base metal veins were formed.

**Cleavage:** Though on a local scale, cleavage is axial planar, Davies (1933) noted that, on a wider scale, axial planes of folds and cleavage are oblique to each other. Cleavage is best developed in the black shale and banded black shale lithologies and has the appearance of a closely spaced cleavage rather than a truly slaty cleavage. Only one phase of cleavage development is present, and microscopic study reveals no evidence of later deformation.

### Nature of the Mineralization (Table 2)

#### *The Roman lode*

The main target for mining at Dolaucothi was the Roman lode (Fig. 7A) which directly underlies the Ogofau pit and the Cothi valley to the southwest. The lode was intersected in New Shaft (see Fig. 4) at a depth of 25.3 m and consisted of a 1.2-m-thick quartz vein containing pyrite, arsenopyrite, and minor amounts of galena. The length-weighted average assay value was 19.14 g/metric ton. Figure 8 presents a cross section of this vein based largely on descriptions by Holman (1911). The corrugated hanging wall is overlain by 7 to 15 cm of soft dark clay whereas the footwall is underlain by 30 cm of shale. This shale has a cleavage parallel to the main vein and contains small quartz stringer veins. It is underlain, in turn, by a 10-cm-thick vein containing laminated quartz and pyrite

TABLE 2. Summary of Mineralization Styles at Dolaucothi

Mineralization style	Description
Roman lode	Flat-lying quartz reefs up to 6.0 m thick, perhaps controlled by a thrust plane
Footwall quartz leaders	A series of en echelon quartz veins apparently emanating from the base of the Roman lode and terminating in a downward direction
Pyritic shales	Impregnations of euhedral and framboidal pyrite concentrated along bedding planes in banded black shale
Footwall stringers veins	Thin irregular to pygmatic veinlets of pyrite, quartz, and carbonate in southeasterly dipping swarms; only found in shales in the structural footwall of the Roman lode
Shear-zone veins I	Gently inclined stacks of podiform quartz veins associated with heavily sheared and pyritized shale
Shear-zone veins II	Steeply inclined irregular veins with abundant sulfide, which are also associated with sheared and pyritized shale
Lead lode	Fault gouge with impregnations of argentiferous galena and minor amounts of sphalerite

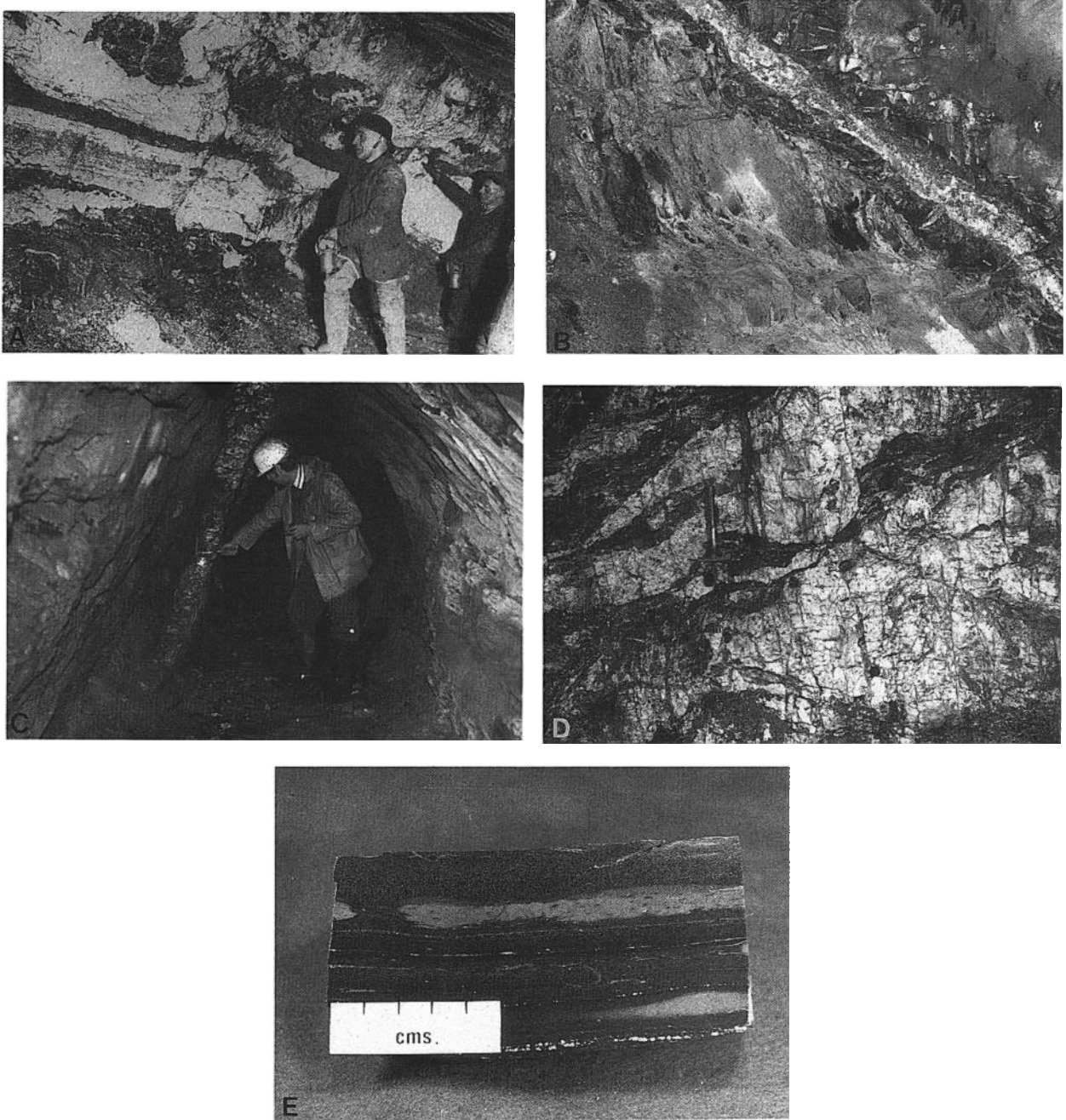


FIG. 7. Auriferous quartz veins. A. Roman lode on the 260-ft level (photographed in 1936). B. Sulfide-rich quartz stringer vein with associated wall-rock alteration (Five-ways, Mitchell adit). C. Planar quartz vein (Five-ways drive south, Mitchell adit). D. Gently inclined quartz pods separated by partings of heavily sheared pyritic shale with abundant hydromuscovite and quartz stringers (Mill adit). E. Typical pyritic shales showing disseminations, bedding plane concentrations, and lenses of pyrite. F. Pyritization of shale associated with the upward termination of a quartz vein. G. Euhedral crystals of pyrite on a bedding plane in black pyritic shale. H. Pyritic shale containing bedding plane concentrations and randomly dispersed laths of arsenopyrite. I. Quartz vein containing clasts of pyritic shale with porphyroblasts of arsenopyrite.

and grading 17.1 g/metric ton of gold. This package of sheared shale and quartz veins is itself underlain by a zone containing numerous quartz leaders de-

scending from the Roman lode above and dipping at approximately  $40^{\circ}$  to  $50^{\circ}$  southeast. A section of a crosscut on the 100' level drawn by Holman in 1909

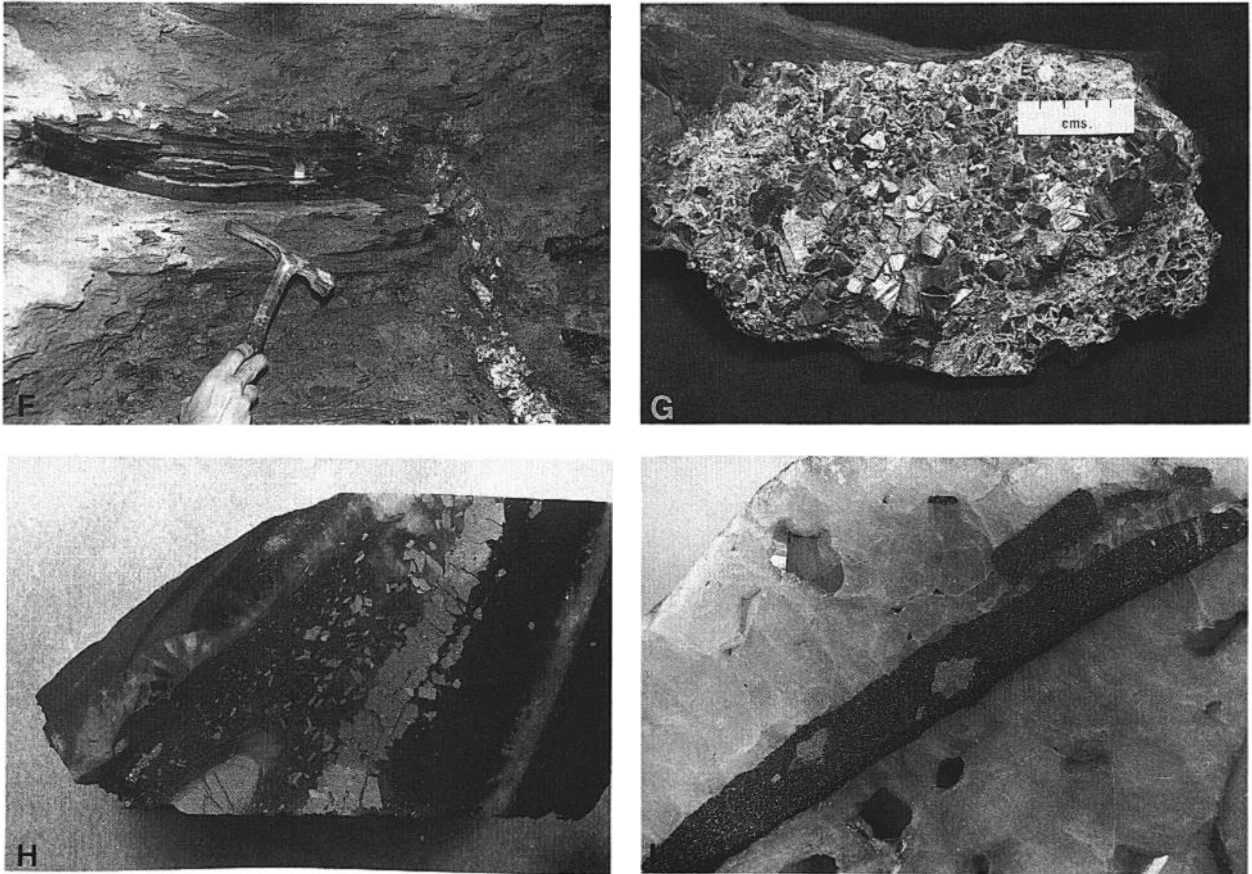


FIG. 7. (Cont.)

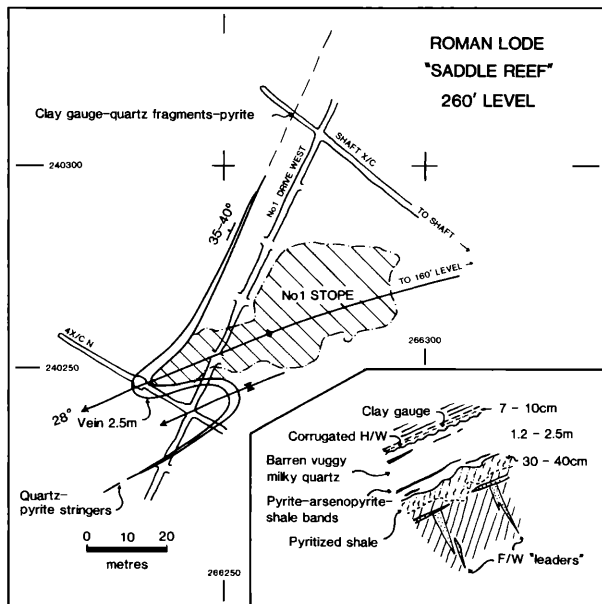


FIG. 8. Plan and diagrammatic section of the Roman lode (for location see Fig. 4).

(Fig. 9) shows an extensive network of quartz stringers and pyritic shale horizons, as well as the quartz leaders. Assays quoted on this unpublished section range from 3 to 35 g/metric ton. Some doubt exists concerning the accuracy of these grades because resampling in 1933 gave lower values.

A composite level plan of the mine workings as of 1939, together with information gleaned from Nelson (1944), suggests that the Roman lode is a classic saddle reef with an S fold structure on each level (see Fig. 8). Nelson records 2.4 m of quartz around the nose of the structure, underlain by 30 to 40 cm of patchily impregnated pyritic shale. Stopping during the period 1937 to 1938 generally followed the crest of the main anticlinal fold as it plunged at 28° on a bearing of 255° down to the 360-ft level. Average stope strike widths were 25 m (Fig. 8) and back heights ranged between 1.2 and 6.0 m. No stopping took place below the 360-ft level due to the uncertain location of the lode at greater depths and also to the lack of capital for further underground development.

Because the underground workings leading from the 150-m-deep New Shaft are flooded, the structural

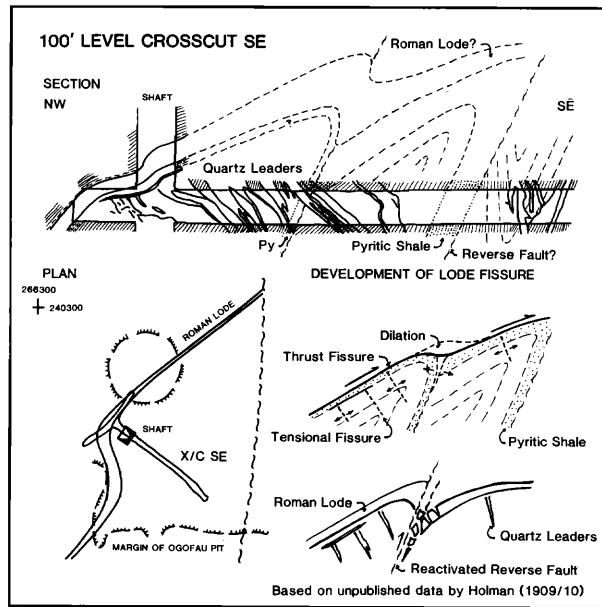


FIG. 9. An interpretative cross section of the Roman lode and underlying quartz leaders (after Holman, 1911).

control of the Roman lode can only be determined by interpretation of descriptions in the literature and old mine reports. The following facts are pertinent:

1. The hanging-wall formations are relatively undisturbed and conformable with the lode.
2. Footwall formations are intensely folded, fractured, and veined.
3. To the northeast, the lode passes into a pyritic gouge, possibly a low-angle fault dipping at  $38^\circ$  to the northwest; to the southwest, the lode passes into a shale-quartz complex in which both shale and quartz are contorted and fractured.
4. Fold hinges contain saddles of quartz which are generally barren and vuggy, but they are enriched in sulfide and gold where there are shale partings.
5. Fractures adjacent to sheetlike or saddlelike masses of quartz are lined with sulfides, quartz, and hydromuscovite.

Brammall et al. (1937) refer to the Dolaucothi lode zone as a mineralized thrust zone transgressing the lower Llandoveryan (basal Silurian) and the underlying Ordovician. The present authors suggest that this is a better explanation for the existence of the Roman lode than the simple saddle reef hypothesis. A possible interpretation of the geology recorded in the lower portion of Figure 9. This interpretation would thus require that the lode fissure be a thrust plane and would date the Roman lode and its footwall leaders as postfolding. The leaders would then be interpreted as extensional shear gash veins produced by the shear couple which

initiated the thrust. Structural culminations, in which a thicker vein could be emplaced, might then be explained in terms of deviation of the thrust as it passed through the hinge zones of anticlinal folds. The zone of complexity and disruption to the southwest of the anticlinal nose (i.e., in the supposed syncline) is then best explained in terms of a later crosscutting fault and associated drag folding.

In 1937 unpublished consultancy reports placed the estimated available reserves in the Roman lode at 150,000 metric tons grading between 8.5 and 17 g/metric ton. However, W. J. Hughes (unpub. rept., 1939) estimated that the total production from this source was only 18,000 metric tons at 6 g/metric ton, yielding approximately 100 kg of gold.

### Pyritic shales

Open-pit (Roman) and adit mining (late 19th and early 20th century) within the footwall of the Roman lode, together with recent drilling by the University of Wales, College of Cardiff, has revealed the existence of numerous bands of heavily pyritized shale ranging from a few centimeters to 3 m in thickness. Though mine assay plans show pyritic shale units grading between 5.1 and 17.1 g/metric ton over 0.6 to 1.8 m, little attempt was ever made to mine these shales even though Nelson (1944) refers to a "Pyrite Lode."

Pyrite may occur as weak disseminations of fine (<1 mm) euhedral grains or slightly richer seams following bedding traces. It may appear locally in dense concentrations (>80% pyrite) in bands parallel to bedding in the shale (Fig. 7E). These bands may show grain size variations reminiscent of graded bedding and also contemporaneous slumping and load casting. These features were initially explained by the authors as being products of syngedimentary exhalative processes.

Recent remapping of surface and underground exposures by the authors has revealed that, though these pyritic horizons are apparently folded with the host shales and are dislocated by shear zones and reverse faults, they terminate along strike and downdip without apparent reason. Careful mapping of the limits of pyritization also reveals that, on a local scale, they are transgressive to bedding. Figure 7F shows a band of intense pyritization along bedding associated with the termination of a quartz vein. However, this feature is developed only on one side and can be traced laterally for a distance of approximately 1.5 m. Elsewhere, pyrite, which is normally in banded black shale lithologies, may be distributed upward into much siltier units (the banded black shales and siltstone unit and the shale and siltstone unit). In freshly blasted underground exposures, pyritization can be seen to be accompanied by abundant quartz stringers. Such

relationships are not compatible with a syndimentary or syngenetic origin for the pyrite.

The nature of the pyritic shales can be determined more precisely by study of drill cores from the 12 holes drilled to date on the Dolaucothi lode zone. Pyrite can occur in many different modes, including: (1) dull fine-grained bands less than 1 cm thick separated by finely disseminated pyrite; (2) lenses or nodules (5 mm–4 cm long) of fine-grained pyrite which can be ascribed to accretionary processes—these accretions may have sharp or diffuse margins, internal syneresis cracks, peripheral halos of disseminated pyrite, and arcuate dilatation openings, infilled with quartz and carbonate, around those margins in the direction of cleavage; (3) bright massive sulfide bands, 2.5 to 7 cm thick, with pyritic halos and internal quartz veins up to 2 cm thick which are truncated by the outer surfaces of the band and which appear to fill in pull-apart structures; (4) diffuse clouds containing variable concentrations of pyrite (20–100%) and clearly transgressing bedding; (5) marginal selvages to pyrite-lined fractures or to later quartz, carbonate, pyrite, arsenopyrite veinlets; and (6) coarse crystal aggregates along bedding planes (Fig. 7G).

Though pyrite normally occurs without other sulfides, it may also be accompanied by arsenopyrite, a late-stage product of sulfidation. Arsenopyrite occurs as large crystals (2 mm–2 cm) or aggregates in siltier (more permeable) bands; as randomly distributed lath-, diamond-, or wedge-shaped crystals (1–3 mm long) distributed throughout the pyritized shale, perhaps with a weak bedding plane control; and as larger euhedra in the proximity of mineralized fractures and veins (Fig. 7H). Pyritic shales are generally intersected by a network of thin irregular to ptigmatic or boudinaged veinlets varying from a fracture-controlled concentration of large pyrite crystals with overgrowths of quartz, carbonate, and hydromuscovite, to vuggy quartz veins (10–20 cm thick) with marginal concentrations of pyrite and arsenopyrite and trace amounts of sphalerite, galena, and chalcopyrite. These veinlets are invariably surrounded by pyrite-arsenopyrite halos, several centimeters wide, which show a marked similarity to the mineralization in the thicker pyritic shale units.

No evidence has been found that cleavage played any role in determining the disposition of the sulfides; indeed, bedding was the dominant control. On the other hand, cleavage has been seen to terminate abruptly against grains of pyrite, and quartz-carbonate pressure shadows, adjacent to pyrite nodules and euhedra of pyrite, are aligned in the direction of cleavage. Some paragenetically early veinlets associated with the pyritic shales are ptigmatic and ruptured, and cleavage traces are bunched and deflected as they pass between the displaced segments of these veins.

All of these features suggest that the maximum stress postdated, or at least overlapped with, this period of mineralization. Most of the main-stage auriferous quartz veins, however, postdate the pyritization since clasts of pyritic shale are found in some of these veins (Fig. 7I).

Microscopically, the disseminated and nodule pyrite consists of equant grains, ranging in size from 5 to 120  $\mu\text{m}$  (Fig. 10B), which are progressively more euhedral as the grain size increases. Small ovoid framboids, 30 to 80  $\mu\text{m}$  in diameter, are also common (Fig. 10A) especially in nodules and in the bands of stoney pyrite (fine-grained sulfidite layers). Large porphyroblasts of pyrite in the shales appear to have grown in situ. They are unrelated to fractures and possess cores rich in silicate inclusions and rims which are clear of inclusions. Galena and sphalerite (with inclusions of chalcopyrite) may be found in the pyrite or within quartz pressure shadows around the margins of the pyrite crystals.

Porphyroblasts of arsenopyrite are developed dominantly in shales containing disseminated pyrite, avoiding the more massive compact pyrite bands or sulfidites. They postdate the pyrite which they have incorporated without replacement (Fig. 10C). The lack of replacement, together with the observation that the concentration and size of these inclusions is slightly less than in the pyritic shale, suggests that arsenopyrite deposition may have overlapped that of the pyrite and was related to the same hydrothermal event. Some of the porphyroblasts are fractured and displaced, and the cavities so produced have been filled in with quartz and/or carbonate. The margins of these fractures are highly irregular or carious. Relict inclusions of arsenopyrite indicate that this sulfide has been corroded or resorbed during the emplacement of the quartz. Other solution cavities have been filled in with quartz and base metal sulfides. Replacement of the host by chalcopyrite and sphalerite has also been observed. Branching veinlets of chalcopyrite, galena, sphalerite, and native gold are also present, suggesting a late-stage remobilization or emplacement of gold along with base metal sulfides.

Large arsenopyrite-pyrite aggregates are also found in the shales which possess an internal banding marked by silicate inclusions (5–25%) aligned parallel to bedding traces in the surrounding shale. These aggregates evidently formed by replacement of the shale in a way similar to the arsenopyrite porphyroblasts, but they lack the inclusions of euhedral pyrite and framboids. They consist of a fine-grained polycrystalline mosaic of (recrystallized?) arsenopyrite in which crystal faces are developed only at the outer margins. The aggregates are cut by fine veinlets containing variable amounts of chalcopyrite, galena, and sphalerite. Large crystals of pyrite are also enclosed and partially replaced by arsenopyrite.

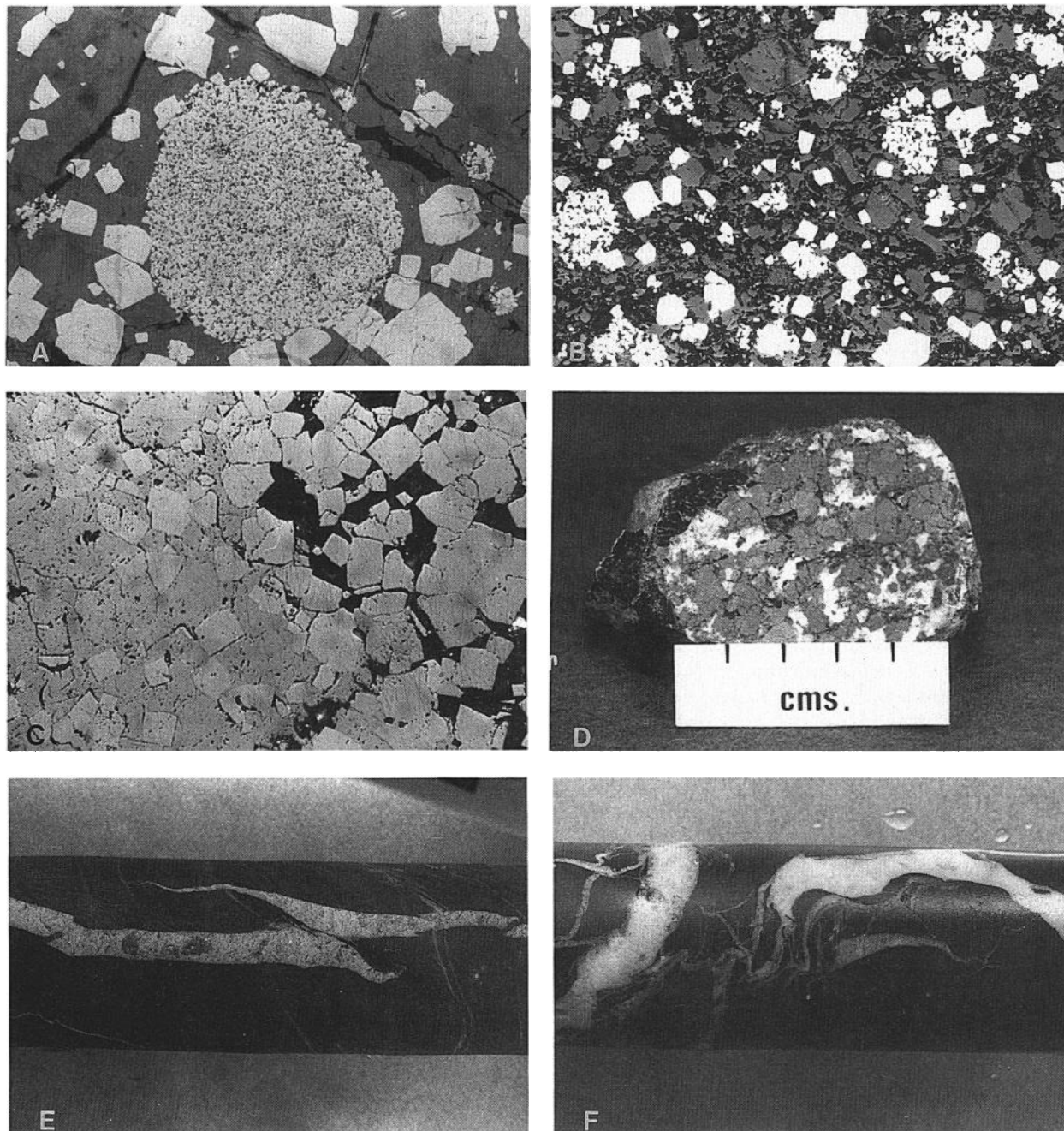


FIG. 10. A. Pyrite framboid in pyritic shale. B. Framboidal and euhedral pyrite in black shale. C. Euhedral pyrite (light gray) enclosed within porphyroblastic arsenopyrite developed within black shale. D. Pyrite and arsenopyrite concentration in planar quartz vein (Mitchell adit). E. Tensional gash veins with visible gold (Allt y Brunant). F. Quartz stringer veins in drill core from the Allt y Brunant prospect.

### Vein Systems

#### *Footwall stringer veins*

The dominant veins in terms of abundance are those referred to earlier which cut the footwall formations of the Roman lode and which are intimately related

to the pyritization of these shales. These veins occur in swarms which dip between  $45^{\circ}$  and  $75^{\circ}$  to  $150^{\circ}$  to  $160^{\circ}$  (Annels and Hellewell, 1988). Many of these veins are somewhat irregular to ptigmatic in form, whereas others are sigmoidal en echelon veinlets (Fig. 10E and F). All are emplaced in strongly cleaved to

sheared shales and have been affected by tectonic activity to varying degrees. Quartz is strained and carbonate is totally recrystallized. Where veining is particularly intense, several phases of crosscutting veins can be recognized. Some veins are little more than mineralized fractures or microveinlets, whereas others are fracture-controlled aggregates of coarsely crystalline pyrite (1–2 cm thick) together with interstitial quartz and carbonate. Others consist of vuggy, milky-white quartz (10–20 cm thick) with concentrations of sulfides, shale clasts, and interstitial masses of pale yellowish-brown carbonate and hydromuscovite at the margins (Fig. 7B). Strong concentrations of carbonate are present where there are shale clasts in veins. Microveinlets of hydromuscovite and carbonate branch out from these veins into the adjacent wall rock. Though pyrite is the dominant sulfide, many veins also contain auriferous arsenopyrite and trace amounts of base metal sulfides. All veins are clearly the product of tensional stress and are not directly related to reverse faulting.

Microscopic study of the arsenopyrite-bearing veins show that some have undergone sequential development by stoping and reopening, causing the fragmentation and veining of early arsenopyrite crystals by quartz and, in some cases, by galena. However, some irregular xenocrystic grains of arsenopyrite contain silicate inclusions and show evidence of marginal and internal dissolution.

#### Planar veins

A set of subparallel quartz veins, of limited strike length, occur within a 45-m-wide northeasterly trending zone aligned approximately along the updip extension of the axis of the Roman lode. This zone passes through the Mitchell adit level and its immediate sublevel and extends upward, via the Mitchell stopes, into an old Roman excavation known as the Mitchell pit (Figs. 4, 11A and B). This vein system terminates downward because, in the underlying Long adit 24 m below, no equivalent veins are present. These veins are evidently the equivalent of the “footwall quartz leaders” which old reports describe from the 100-ft level and which occur beneath the Roman lode. At the surface in the Mitchell pit, this zone is bounded by reverse faults (A and C in Figs. 5 and 11B) which interrupt the strike continuity of the veins both to the north and to the south. The last period of reverse faulting must, thus, have postdated vein emplacement, a relevant fact for the interpretation of the Roman lode geology, as discussed earlier.

The Mitchell adit veins show variable easterly dips (between 42° and 72°, becoming steeper in the sublevel) whereas the strike changes from south to north from 52° to 334° as the footwall of the northern steep-dipping reverse fault (C in Fig. 5) is approached.

The veins vary in thickness from a few centimeters

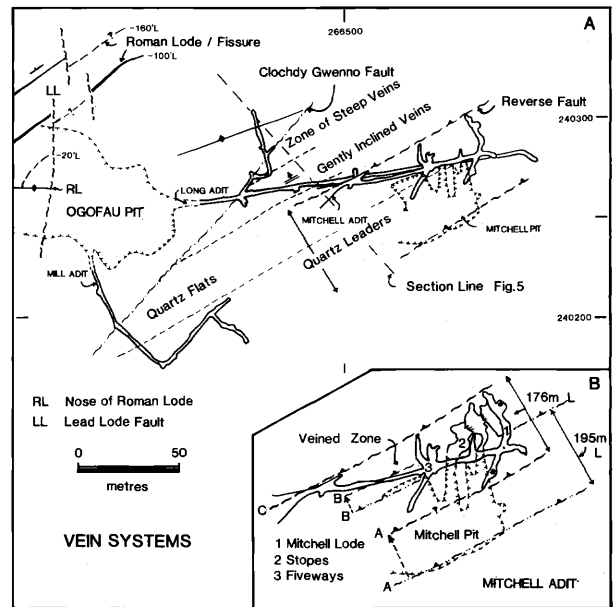


FIG. 11. Distribution of vein systems adjacent to the Ogofau pit.

up to 1 m and many show a downward or lateral pinch out into a series of en echelon veinlets (Figs. 7C and 12). Some veins may have highly irregular margins, with apophyses penetrating the adjacent country rock whereas others split into a series of thin stringer veins. The main Mitchell lode is a composite vein system with individual veins separated by thin shale partings. The rocks adjacent to these veins rarely show evidence of strong wall-rock alteration unless the vein is heavily charged with sulfides. Bedding planes adjacent to the veins are often deflected, thus indicating reverse fault movement on the host fissure. However, there is no displacement of beds on either side and this feature is due to an inclined tensional fissure cutting across bedding which has an opposing dip direction. Fluid pressures allowed continued downward propagation of the fissure and the upward or downward deflection of bedding immediately adjacent to the fissure. The downward attenuation of veins is thus accompanied by the disappearance of this apparent drag.

The veins contain coarsely crystalline drusy quartz and only rarely is sulfide mineralization seen. The main exceptions are thin veins and associated sigmoidal gash veins in the central section of Mitchell adit known as “Five-ways” (Fig. 11B). Here, a lamellar structure is apparent due to bands of pyrite and arsenopyrite alternating with bands of quartz and carbonate. These veins range from 5 to 30 cm in thickness and possess grades of up to 30 g/metric ton over these widths, with additional values in the adjacent shales. These shales show a characteristic



FIG. 12. A planar quartz vein in the Mitchell adit showing downward thinning. Note deflection of bedding adjacent to vein.

darkening and the development of a soapy feel, largely due to hydrothermally introduced hydromuscovite (illite). Locally pyritization along bedding planes is evident adjacent to the veins and thus, vein emplacement was preceded by, or accompanied by, wall-rock impregnation.

The northern reverse fault exposed in the entrance to the Mitchell adit (Figs. 4 and 5) can be traced down into the Long adit where its location is marked by heavily sheared and disrupted shales and subvertical veins. Such veins are unusual at Dolaucothi and may represent a late stage of veining, postdating reverse faulting. A westerly dipping fault, exposed in the shaft between the Long and Mitchell adits, may also explain the absence of the well-developed, Mitchell lode in the Long adit. The information presented above thus implies that the Mitchell veins are directly related to the Roman lode and that originally this saddle reef would have been positioned directly above these veins and above the present topographic surface. The Clochdy Gwenno fault (Fig. 5) is responsible for the preservation of the Roman lode on its downthrown northwestern side.

### *Shear-zone vein systems*

A description of these veins is based on exposures in the Long and Mill adits, together with workings in and around the Davies cutting and two surface drill holes (Fig. 4, M1 and M2). These veins are truncated to the northwest by the later Clochdy Gwenno fault and they represent an entirely different style of mineralization from that described in the Mitchell adit, but they are contained within the same zone, at a lower structural level.

The veins are exposed in a northeasterly striking section, 25 m wide, in which the shales have been intensely sheared and disrupted, so much so that very little core is recovered in underground drill holes, other than sections of massive quartz. The shear zone can be subdivided into two portions; a northwestern and a southeastern segment (Fig. 11A). The northwestern portion is at least 10 m wide and contains a chaotic assemblage of steeply dipping subparallel veins, large irregular bosses of barren, white vuggy quartz, and horseshoe-shaped veins. The associated sheared graphitic shales contain a network of stringer veinlets containing abundant pyrite, hydromuscovite, cookeite, and quartz; pyrite-arsenopyrite impregnations are also common. The subparallel veins are commonly less than 20 cm thick and dip to the northwest at between 65° and 90°. Locally, they may constitute 20 to 40 percent of the rock mass in this zone and are important because they are heavily charged with pyrite and arsenopyrite, either as central ribs or as scattered grains and aggregates. Some veins have sigmoidal forms, but others terminate abruptly against upper and lower slip planes (thrusts?) against which they are inclined at approximately 40°. Assays through this zone generally range between 3 and 13 g/metric ton Au.

The southeastern portion of the zone in the Long adit and in the Davies Cutting adits contains gently inclined veins or lenticular pods which dip between 10° and 30° to the northwest. These veins are typically less than 50 cm thick, though they may locally swell to as much as 1 m, and individual veins can only be traced for a few meters along strike or downdip. They are stacked one on the other and are separated by thin partings of heavily sheared and pyritized shale injected by abundant quartz, pyrite, and hydromuscovite stringer veinlets (Fig. 7D). At the contact between the two zones in Long adit, there are two superimposed quartz reefs which have been stoned and which dip at approximately 25° to the southeast. Both the upper reef (0.8 m thick) and the lower reef (1.6 m thick) possess many of the characteristics described for the Roman lode but they have reversed dips.

In the Mill adit, only the flat-lying veins are present over a section 16.5 m wide immediately adjacent to the Clochdy Gwenno fault. These veins have a dip of 5° to 10° to the southeast and may form part of a

third zone to the southeast of the two main zones described above. Similar veins in the Long adit, close to the internal shaft, may constitute a zone 25 m wide (Fig. 11A). The veins cut tight asymmetric folds and are, thus, later than the main stage of folding. A relationship with reverse faults is implied. Thus, the flat-lying veins are thought to be controlled by tensional fissures associated with a steep-dipping (80° NE) reverse fault, perhaps fault C observed in the Long adit.

### Mode of Occurrence of Gold

Gold is associated with a variety of different styles of sulfide mineralization but has not been detected in pygmatic pyrite (quartz-carbonate) veins, in finely disseminated pyrite impregnations with framboids, or in late-stage siderite, quartz, and base metal sulfide veins. It reaches its highest tenor in shales containing massive to banded aggregates of mixed sulfides containing minor amounts of quartz-carbonate gangue, in sulfidite bands, and in heavily pyritized shales with abundant arsenopyrite porphyroblasts. These shales may be closely associated with thin quartz, sulfide, carbonate veins containing in excess of 10 g/metric ton Au. Thick veins with strong concentrations of pyrite may lack arsenopyrite and microscopically visible gold but still assay in excess of 30 g/metric ton. The gold must be submicroscopic or in solid solution in the pyrite. Thick veins of coarsely crystalline quartz are usually barren or of low grade (<1 g/metric ton).

Generally gold occurs as sulfide-locked grains which vary in size from microscopic to grains which are just visible with the naked eye (200  $\mu\text{m}$ ); most fall in the range 15 to 30  $\mu\text{m}$ . Free gold is rare and only four grains in the range of 1 to 2 mm have been recorded in drill core; all were in small tensional gash veins. Gold has been observed in the following locations: (1) in quartz + carbonate fracture infillings in pyrite and arsenopyrite where it forms an outgrowth from the margins of the ruptured sulfide, (2) as attachments on the margins of grains of arsenopyrite (Fig. 13), (3) at intergranular boundaries in aggregates of pyrite and arsenopyrite or within arsenopyrite porphyroblasts containing pyrite inclusions, (4) as small rounded or spindle-shaped inclusions in both pyrite and arsenopyrite, especially close to the outer rim of the host, (5) as the sole infilling of branching hairline fractures in sulfides, (6) as intimate intergrowths with chalcopyrite, sphalerite, and galena in microveinlets cutting arsenopyrite, or with galena cementing fragmented grains of arsenopyrite, and (7) as scattered grains following inclusion trains in sulfides.

These observations strongly suggest that the gold was exsolved from hydrothermally precipitated arsenopyrite and pyrite, especially close to, or at, grain

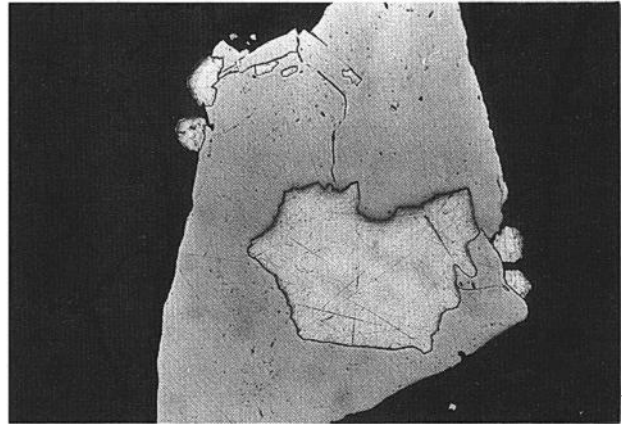


FIG. 13. Crystal of arsenopyrite with attachments and inclusions of gold (large grain 400  $\mu\text{m}$  across).

boundaries or internal microfractures, when the host mineral tried to rid itself of impurities (Au and Ag).

### Mineral Chemistry

Electron microprobe analyses of arsenopyrite and associated grains of gold revealed little variation in composition which could be related to the mode of occurrence of gold. Arsenopyrite has an average composition of 34.8 percent Fe, 21.5 percent S, and 43.7 percent As (16 analyses), and the associated gold a fineness ( $\text{Au} \cdot 1,000 / (\text{Au} + \text{Ag})$ ) of 785 ( $\sigma = 9.4$ ). These gold values are admittedly on a limited number of analyses (7) and the picture could change as additional information is obtained. On the other hand, pyrite in the late-stage quartz veins was significantly enriched in arsenic (2–2.5%) compared with that occurring as disseminations in shales (0.4–1.9%).

Carbonates in the auriferous veins are pale buff colored and have compositions in the field of magnesium-rich ankerite. Late-stage carbonate, in post-cleavage base metal sulfide-bearing veins, lies in the field of siderite.

Hydromuscovite, a white to greenish-white, talc-like mineral, first reported at Dolaucothi by Brammall et al. (1937), is found in the Roman lode, in quartz-pyrite veinlets and in association with pyrite impregnations. Brammall et al. record that a typical sample of broken ore from the Roman lode on the 420-ft level contained 6 percent hydromuscovite and that this mineral contained approximately 8 percent  $\text{K}_2\text{O}$  and 0.22 to 0.46 percent  $\text{Na}_2\text{O}$  (see lithogeochemical analyses summarized later). The mineral was identified by Nagelschmidt (1937) as 1M illite with a composition approximating  $\text{KAl}_2(\text{Si}_3\text{AlO}_{10})(\text{OH})_2$ . However, XRD analyses undertaken for this paper have identified this mineral as a 2M1 illite, and XRF analyses gave slightly lower  $\text{K}_2\text{O}$  values (6%) and higher

Na<sub>2</sub>O values (1.26%) than those reported by Brammall et al. (1937).

Brammall et al. (1937) also reported the occurrence of the lithium-bearing silicate, cookeite, a chlorite-like mineral with an approximate composition of LiAl<sub>4</sub>Si<sub>3</sub>AlO<sub>10</sub>(OH)<sub>8</sub>. Their analyses of a bulk sample of ore from the 420-ft level indicated 0.01 percent cookeite and that this cookeite contained 2.45 percent Li<sub>2</sub>O. Cookeite was not found at the surface and was described as rare in the upper levels of the mine. Where it did occur, it lined small cavities, fractures, and shear planes in the quartz lodes and pyritic shales and was thus a late-stage hydrothermal introduction into the lode zone. Brammall et al. relate cookeite to low-temperature hydrothermal fluids, perhaps derived from a granitic or granodioritic magmatic intrusion at depth. They point to its increasing abundance, along with hydromuscovite, in the lower levels of the mine.

The authors also collected samples of hydromuscovite from fractures in pyritic shale exposed in the Davies cutting on the eastern margin of the Ogofau pit. XRD analyses confirmed the existence of hydromuscovite but also detected cookeite, indicating that this mineral is perhaps more common nearer the surface than was first thought.

#### Host-Rock Lithochemistry

Detailed lithochemical analyses of the country rocks from the Dolaucothi lode zone were undertaken by Tater (1975) and reviewed by Steed et al. (1976). This work revealed that, in hydrothermally altered black shales adjacent to the lodes and also in pyritic shales, the concentrations of Pb, As, Rb, and K were considerably enhanced compared with their lateral equivalents beyond the lode zone, whereas Zn and Mn were depleted. Lithium showed enrichment only in those shales adjacent to the quartz veins, perhaps reflecting the presence of cookeite. Systematic sampling underground confirmed these enrichments and depletions and indicated that a low-intensity Rb (and K<sub>2</sub>O) anomaly is centered on the lode zone. Adjacent to individual veins, rubidium values decline from peak values as high as 449 ppm Rb to the local background levels of 310 ppm over distances of approximately 12 m. This background level is itself an abnormal level since the regional background is 245 ppm, indicating an even broader anomaly as originally proposed by Al-Atia and Barnes (1974).

A study of drill core samples of altered shales from the vicinity of the quartz veins showed that these shales contained enhanced levels of Na<sub>2</sub>O (mean = 0.87 vs. 0.66%) and K<sub>2</sub>O (5.12 vs. 4.05%) compared with unmineralized and unaltered shales. These values can be ascribed to the presence of hydromuscovite in these rocks. CaO shows a slight increase

(0.30 vs. 0.22%) whereas the mean MgO value displays a significant decrease (from 1.36 to 0.82%). Recalculation of the analyses for the pyritic shales on a sulfide-free basis shows that K<sub>2</sub>O is only weakly enhanced but that CaO is markedly higher (0.87%, accompanied by a drop in MgO to 0.67%). This calcium content could be interpreted as resulting from the replacement of host-rock chlorite by illite and carbonate, both of which are conspicuous in thin sections.

#### Stable Isotope Studies

##### Sulfur

A total of 41 sulfide samples have been analysed for  $\delta^{34}\text{S}$  (Table 3). Samples were chosen to cover the types of mineralization and paragenetic ages present. With the exception of the late-stage veins, the results are remarkably uniform, with a mean  $\delta^{34}\text{S} = -4.48$  per mil and a range of  $-3.27$  to  $-6.85$  per mil.

##### Oxygen and carbon

A total of eight  $\delta^{18}\text{O}$  and  $\delta^{13}\text{C}$  analyses were obtained on carbonate samples (Table 4). The first two analyses were performed on unmineralized shales containing minute spots of carbonate whereas the following four were on auriferous veins and the last two on late-stage veins. The surprisingly heavy  $\delta^{18}\text{O}_{\text{SMOW}}$  value of the first sample was confirmed by repeated analyses and remains an enigma. However, the second shale value (16.11‰) falls within the range of the auriferous vein carbonate (mean  $\delta^{18}\text{O}_{\text{SMOW}} = 16.25\text{‰}$ ,  $\sigma = 0.14\text{‰}$ ). The two late-stage veins possess a slightly heavier value averaging 17.87 per mil, perhaps due to formation at lower temperatures. Friedman and O'Neil (1977) state that the fractionation equation for the oxygen pair calcite-H<sub>2</sub>O is  $2.78 \times 10^6/T^2 - 2.89$  (where T is in °K) for the temperature range 0° to 500°C. If this equation is applied for an average depositional temperature of 400°C (see later), then the isotopic composition of the fluid in equilibrium with calcite would be 3.25 per mil lighter than that of the calcite itself. Using the carbonate data in Table 4, the isotopic composition of the main-stage vein fluid would thus have been close to a  $\delta^{18}\text{O}_{\text{SMOW}}$  value of

TABLE 3. Sulfur Isotopes

Sulfide type	$\delta^{34}\text{S}$		No. of samples
	Mean	$\sigma$	
Pyrite nodule	-4.39	0.99	5
Disseminated pyrite	-4.69	0.85	9
Early pygmatic vein pyrite	-4.08	0.42	3
Main-stage vein pyrite	-4.15	0.66	7
Aggregates of arsenopyrite	-4.61	0.34	6
Arsenopyrite porphyroblasts	-4.55	0.12	4
Late-stage pyrite	-2.35		2
Late-stage chalcopyrite	-0.04		2
Late-stage galena	-7.08		2
Late-stage sphalerite	-4.75		1

TABLE 4. Carbonate Isotopes

Carbonate type	$\delta^{13}\text{C}_{\text{PDB}}$	$\delta^{18}\text{O}_{\text{PDB}}$	$\delta^{18}\text{O}_{\text{SMOW}}$
Shale	-16.24	-1.66	28.66
Shale	-16.75	-13.84	16.11
Main-stage vein	-15.60	-13.73	16.22
Main-stage vein	-14.80	-13.49	16.47
Main-stage vein	-15.47	-13.88	16.07
Main-stage vein	-14.68	-13.70	16.25
Late-stage vein	-13.68	-12.17	17.83
Late-stage vein	-13.57	-12.09	17.91

13 per mil. However, the vein carbonate is an Mg ankerite, for which fractionation data are not available. Dolomite-H<sub>2</sub>O fractionation is, however, approximately 3 per mil greater than that for calcite (Olson, 1984) and this can thus be used to assign a value of 10 per mil for the fluids precipitating the ankerite.

In all cases, the  $\delta^{13}\text{C}_{\text{PDB}}$  values are light and reflect a strong organic <sup>12</sup>C input, supporting a source in the host-rock shales.

### Geothermometric Studies

#### *Paleotemperatures—geothermal gradients*

Estimates of the thickness of the sediments (Ordovician to lower Downtonian) deposited on the Cambrian in mid-Wales by the onset of the Caledonian orogeny have been reviewed above. For the Dolaucothi area, thicknesses may have been between 7 and 8.5 km (P. D. Lane and R. E. Bevins, pers. comm., 1982), whereas the combined thickness of the rocks overlying the mineralized strata are estimated to have been 5 to 6 km. Table 5 represents a compilation of possible paleotemperatures based on a range of possible geothermal gradients (25, 30, and 40°C/km) and ambient surface temperatures of 18°C.

#### *Paleotemperatures—conodont color alteration indices*

Color alteration index values for conodonts extracted from rocks of Llandeilo to Bala age in central Wales were uniformly equal to 5 (Bergstrom, 1980), indicating a temperature range between 300° and 400°C. This range compares with index values of 1 to 1.5 (50°–90°C) for the Welsh borderlands outside the Caledonide belt. Bergstrom states that index values of 5 are difficult to explain in terms of overburden thickness and that abnormal heat flow must be considered in response to volcanism and the effect of the orogeny itself. Table 5 shows that a 40°C/km gradient would meet this requirement if the depths were at the upper end of the estimated range.

#### *Paleotemperatures—metabasite metamorphic facies*

Metamorphic facies within the basal Ordovician of Wales (Bevins et al., 1981; Bevins and Rowbotham,

1983) show a change from diagenetic, around the margins of the Caledonide belt, through anchizone to greenschist toward central, but localized, areas beneath the axis of the orogen. This change is approximately compatible with that reflected by color alteration index values higher in the succession. Robinson and Bevins (1986) suggest, on the basis of clay mineral and metabasite assemblages, that this reflects a temperature range of 150° to 400°C for the Welsh basin. On the basis of their study, any basal Ordovician volcanics present beneath Dolaucothi would be expected to lie close to the transition from pumpellyite-actinolite at the top of the anchizone facies to pumpellyite-prehnite at the base. Pumpellyite-quartz veins are present to the northeast in the Built Wells volcanics. A burial depth of 7 to 8.5 km would give a lithostatic pressure of 2 to 2.4 kbars at this level and the temperatures indicated by the metamorphic facies can be estimated, since prehnite and pumpellyite are stable up to 300° to 320°C at 2 kbars, depending on the iron content of the system (Liou et al., 1985), whereas the assemblage chlorite + pumpellyite + actinolite + quartz is stable between 260° and 370°C above 2.5 kbars. Thus, a range of 300° to 350°C seems justified. This range is compatible with the values of 298° to 358°C calculated for the estimated depths for a gradient of 40°C/km. This thermal gradient agrees with that independently calculated by Robinson and Bevins (1986) for the Prescelly Hills in Pembrokeshire where the metabasite assemblage actinolite + epidote + pumpellyite + prehnite, on the basis of data from Liou et al. (1985), indicates gradients as high as 42°C/km.

#### *Paleotemperatures—illite crystallinity*

XRD analyses, by the authors, of Ordovician shale from the axial zone of the Tywi anticline yielded illites with a Kubler crystallinity index (K.I.) of 0.26 to 0.34 (Kubler, 1967), indicating a middle to upper anchizone range. However, the shales on the Ordovician-Silurian contact on the flanks of the Tywi and Cothi anticlines yielded values averaging 0.184, indicative

TABLE 5. Calculated Paleotemperatures

	Gradient °C/km	Burial temperatures (°C)	
		7 km (min)	8.5 km (max)
Basal Ordovician	25	193	230.5
	30	228	273
	40	298	358
		5 km (min)	6 km (max)
Ordovician-Silurian contact	25	143	168
	30	168	198
	40	218	258

of greenschist facies. Samples from the same horizon at Dolaucothi gave even lower values (avg 0.172), indicating that stratigraphically younger shales in this area were subjected to higher temperatures. Regional investigations by Robinson et al. (1980) indicate a middle to upper anchizone facies for the basal Ordovician in western Wales and greenschist facies for the underlying Middle and Lower Cambrian rocks. Robinson and Bevins (1986) suggest an upper anchizone facies for the Cothi anticline (K.I. = 0.18–0.34) but a lower anchizone (K.I. = 0.34–0.43) for that portion of the Tywi anticline which coincides with the Tywi lineament. Although the suggested metamorphic facies for the area differs, there is general agreement that the rocks at Dolaucothi are of a higher metamorphic grade than surrounding rocks, despite their higher stratigraphic position. Robinson and Bevins (1986) also state that the metamorphism was of a low-pressure type normally characterized by high geothermal gradients and largely produced by depth of burial rather than deformation. They also suggest that a 40°C/km gradient may have existed in the central portion of the Welsh basin. This conclusion implies that high heat flux postdated the folding, especially in the synclinal areas on the flanks of the Tywi anticline. The location of this anticline may have been controlled by basement faults, such as the Tywi-Pontesford lineaments, allowing the concentration of heat flow in narrow zones along its margins.

#### *Paleotemperatures—fluid inclusions*

Fluid inclusions are relatively abundant in vein quartz at Dolaucothi and all are two-phase liquid-vapor inclusions without daughter minerals. Most inclusions are 10 to 50  $\mu\text{m}$  in size, but examples between 100 and 150  $\mu\text{m}$  are not uncommon.

Standard homogenization and freezing techniques have been applied to drill core samples from the Brunant prospect and the Ogofau pit (Fig. 14A) and to samples from veins in underground and surface exposures (Fig. 14B). They show a wide range of values for both homogenization temperatures (102°–408°C) and salinities (2–18 equiv wt % NaCl).

The mean homogenization temperatures for groups of fluid inclusions from different vein types show an increase from those in barren quartz veins (202°–209°C, but as low as 102°C), through barren hydromuscovite-quartz veins and barren quartz-carbonate veins (197°–215°C), to auriferous, sulfide-bearing veins (190°–408°C). The highest temperatures were found in levels associated with the centrally located Ogofau pit (Mitchell adit, 190°–408°C, with a mean of 281°C, and Long adit, 172°–384°C, with a mean of 270°C) declining at the extremities (mean = 214°C for Brunant, and 232°C for Cwrt-y-cilion). Table 6 summarizes the homogenization temperatures and salinity data. The temperature variations can be re-

TABLE 6. Regional Variations in Homogenization Temperatures and Salinities for the Dolaucothi Gold Lodes

Sample location		Mean of means (°C)	Equiv wt percent NaCl
Northeast	Allt y Brunant	214 (19.9)	10.5–18.7
	Mitchell lode	256 (9.7)	6.4–8.3
Ogofau Pit	Middle-Mitchell adits	280 (19.0)	3.7–14.4
	Long adit	270 (19.6)	2.7–13.7
	Mill adit-Davis cutting	263 (11.4)	5.8–9.9
	Pen-lan-wen-Roman adits	235 (16.1)	5.8–7.5
Southeast	Cwrt-y-cilion	232 (28.4)	2.3–9.7

(10.1)—standard deviation

lated to the occurrence of gold and veining because the highest gold values and the highest degree of quartz veining are where the highest temperatures have been recorded.

The salinity values initially show no convincing relationship to the type of mineralization nor to any regional variations. However, a close scrutiny of the data for the Ogofau pit reveals that the range for the barren quartz veins with abundant hydromuscovite (2–10.9 wt %, with a mean of 7%) is significantly lower than that for other veins (2–15 wt %, with a mean of about 10%). Thus, it is likely that the appearance of hydromuscovite was related to fluids with lower salinities than those associated with sulfides.

The histograms for homogenization temperatures in the Ogofau pit indicate a bimodal population (Fig. 14A), with an overlap of populations at 180°C and modes at 160°C and 220–230°C. The lower temperature population can be explained either by the incorporation of secondary inclusions in the data sets (cf. determinations for the main sulfide-bearing veins; Fig. 14) or by a later low-temperature emplacement of quartz and hydromuscovite. Because field and microscopic evidence suggest more than one period of silica precipitation, the second explanation is preferred.

The homogenization temperatures presented above require correction for depth of burial and salinity (see Potter, 1977). An estimate of the minimum depth of burial of the host rocks (Upper Ordovician/basal Silurian) can be made for the onset of the Caledonide orogeny (5 km), but the true value may be somewhat greater (perhaps 6 km) for reasons explained earlier. Tectonic thickening may further increase the necessary pressure correction. However, minimum temperatures can be determined assuming lithostatic conditions for a 5-km depth (140 MPa). On this basis, the early pygmatic quartz-carbonate-pyrite veins were emplaced at approximately 325°C whereas the main-stage veins were formed from fluids

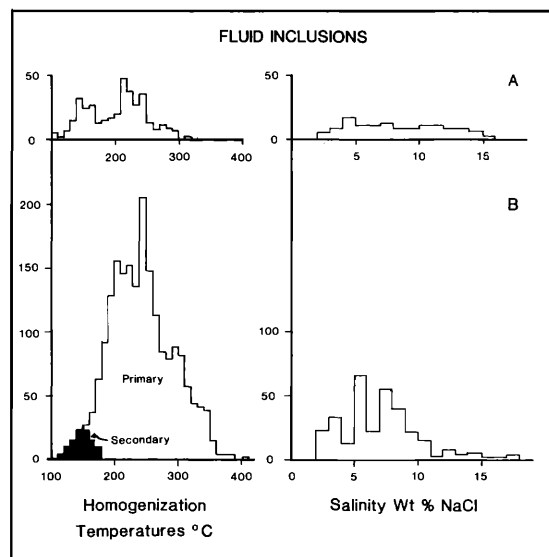


FIG. 14. Histogram of homogenization temperatures and salinities for fluid inclusions. A. Drill core. B. Rock samples.

which changed from close to 345°C at the northeast and southwest extremities of the lode zone, to at least 410°C in the central areas. Individual samples may have been derived from fluids having temperatures as high as 450°C. However, it must be stressed that these values are only estimates and could be lower if conditions were less than lithostatic, or higher, if the depth of burial has been underestimated.

### Discussion

Initially, the apparently stratiform habit of the pyritic shales and the carbonaceous (locally graphitic) nature of the host shales led the authors to consider the possibility that these units were the product of exhalative activity on the sea floor during Early Silurian times. This activity would thus represent the final episode of volcanic activity in this part of Wales. The sulfides were considered syndiagenetic in origin, as were the closely associated pyrite nodules. Framboidal pyrite in the bands of pyrite would reflect low-temperature syndiagenetic sulfides formed under bacterial influence.

Earlier, in the 1930s, strong support was given for a magmatic hydrothermal origin for the shale-hosted pyrite and its emplacement by impregnation and replacement of favorable shale horizons (e.g., Brammall et al., 1937). An epigenetic hydrothermal, but not necessarily direct magmatic, origin for the pyrite is supported by the sulfur isotopes discussed in this paper; there is no evidence for a syndiagenetic origin for the pyrite in the shales. In fact, the similarity of the vein and shale sulfides indicates a common origin. Furthermore, textural relationships, which indicate that the pyrite in the shales was emplaced at an early

stage of orogenesis, coupled with the transgressive nature of the pyritization, make a syndiagenetic origin less likely. All sulfides precipitated from the hydrothermal fluids are isotopically homogeneous, including the pyrite in the shales, and have values which are close to those expected for magmatic sulfur. The limited range of isotopic values is not characteristic of sulfides derived from the reduction of seawater sulfate.

Boyle (1979, p. 398) states that the most likely source of gold is from pyrite and magnetite contained in rocks which were subjected to prograde metamorphism. Particularly favorable source rocks include basic intrusives or volcanics ( $21.6 \times 10^6$  g/km<sup>3</sup>), graywackes and sandstones ( $78.9 \times 10^6$  g/km<sup>3</sup>), and pyritic black shales ( $42.9 \times 10^6$  g/km<sup>3</sup>). Basic volcanics and pyritic black shales are found in the Ordovician of Wales and the Cambrian contains significant thicknesses of graywacke. Though little is known of the Precambrian basement of this area of Wales, it is thought to contain altered volcanics. The magmatic character of the sulfur suggests that it, and perhaps the associated metals, were derived from the metamorphism and leaching of basic volcanics.

Henley (1973) has shown that gold can be transported as a chloride complex and Fyfe and Henley (1973) indicate that the maximum solubility occurs when chloride-bearing solutions have temperatures in the range of 450° to 500°C. These source temperatures agree with the observation that many turbidite-hosted gold deposits are spatially associated with areas which have been subjected to greenschist (particularly mid-greenschist) facies metamorphism (325°–475°C; Mueller and Saxena, 1971).

Fluid inclusion geothermometry indicates that most of the gold mineralization at Dolaucothi was precipitated over the temperature range 350° to 410°C. This is compatible with Fyfe and Henley's (1973) statement that gold is precipitated from chloride solutions over the range of 300° to 400°C. If allowance is made for cooling of the host fluids on their ascent through 2 km of shales, it is unlikely that the source of these fluids was the basal Ordovician where geothermal temperatures are estimated to have been between 298° and 358°C. Greenschist facies metamorphism is known to exist both in the basal Ordovician and in the underlying rocks of west Wales. The above evidence points to an origin for the fluids in the Precambrian basement underlying the southern margin of the Welsh basin, with most of the contained gold from the same source. There is a possibility that some gold was also leached from the basal Ordovician as the fluids ascended into the cover rocks. Though an assumption has been made that the gold was transported as a chloride complex, the possibility that it was in the form of a thiosulfide complex must also be considered. This is an attractive idea because of the

abundance of sulfide that is associated with the gold mineralization. However, the authors have no evidence to prove this hypothesis.

The estimated  $\delta^{18}\text{O}$  values for the fluids (10‰), from which the vein carbonates formed, fall within the fields of both magmatic (6–10‰) and metamorphic waters (5–25‰) (Taylor, 1979) and, thus, shed little light on the precise origin of the fluids. A metamorphic origin is, however, favored. Isotopic analyses for deuterium are needed to constrain the fluid composition more precisely to either metamorphic or magmatic fields. However, the  $\delta^{13}\text{C}$  values are much lighter than those expected from contemporaneous seawater or from fault-controlled alteration of basalts (Groves et al., 1988). Thus, it is suggested that the most of the carbon in the fluid was of organic origin and was derived from the black shales themselves and not from the alteration and metamorphism (decarbonization) of underlying basalts. However, the decrease in  $\delta^{13}\text{C}$  from the shale to auriferous vein to late-stage vein carbonate could be due to an increasing input of magmatically derived carbon with time. Since magmatic  $\delta^{13}\text{C}_{\text{PDB}}$  typically lies between  $-5$  and  $-8$  per mil, mixing with magmatic carbon would result in heavier isotopic compositions.

The Dolaucothi gold deposits possess many of the characteristics of turbidite-hosted gold mineralization elsewhere in the world and particularly that in the lower Paleozoic Meguma Group of Nova Scotia, the Lower Ordovician of Victoria, Australia, the Mesozoic Otago Schists of New Zealand, and the Archean Yellowknife Supergroup of the Northwest Territories, Canada. The nature and genesis of these deposits have been reviewed by Boyle (1986) and other authors in Keppie et al. (1986).

Boyle (1986, p. 2) states that gold deposits in turbidites are "in veins, lodes, sheeted zones and saddle reefs in faults, fractures, bedding plane discontinuities and shears, drag folds, crushed zones and openings on anticlines," all of which are recognized at Dolaucothi. Deposits of this type contain auriferous quartz veins which were emplaced during a period of orogenic deformation and associated prograde metamorphism. Though most were emplaced after the main peak of deformation, following faults (commonly high-angle reverse faults) which transgress fold structures, many have suffered the effects of continued tectonism resulting in the production of quartz boudins and pygmatic veins: the crushing and recrystallization of quartz, the remobilization and reconcentration of earlier gold in fractures, and finally, the emplacement of additional native gold and base metal sulfides by the migration of late-stage fluids—all of these features are recognized at Dolaucothi.

Most turbidite-hosted deposits can be shown to have derived their gold not from the adjacent country rock but from depth during a period of prograde

metamorphism and deformation. The parent fluids are considered to have been trapped at depth during the main period of deformation (e.g., Goldfarb et al., 1986; Paterson, 1986) and released during later rapid uplift of the sedimentary pile. High fluid pressures, generated by great depth of burial, by tectonic compressive regimes, and by thermal expansion during periods of high heat flux, overcame the tensile strength of the rock and allowed the hydraulic propagation and opening of fractures and the rise of overpressured fluids to higher levels in the crust. These low-salinity fluids would be enriched in silica and a variety of elements including iron, the base metals, gold, arsenic, and silver. The most common sulfides found in these deposits are pyrite and arsenopyrite; this is also true for Dolaucothi. However, many turbidite-hosted deposits contain significant concentrations of tungsten, antimony, tellurium, and bismuth, none of which have been detected at Dolaucothi. Other than quartz, the main gangue mineral is an ankeritic carbonate; again, this is true at Dolaucothi. Wall-rock alteration produced by the migrating fluids is reported as being only weak and is represented by narrow zones of mild chloritization, sericitization, and carbonatization, commonly accompanied by disseminations of auriferous pyrite and arsenopyrite. At Dolaucothi, wall-rock alteration is weakly developed and only illitization, sulfidization, and carbonatization have been recognized. There are, however, veinlets and cavity infillings of chlorite which appear to predate the main phases of quartz vein intrusion.

### Conclusions

The following represents an interpretation of the sequence of events which led to the emplacement of the gold mineralization at Dolaucothi and the later modification and displacement of the lode zones.

1. Prograde greenschist metamorphism of the basement during the Caledonian orogeny led to the creation of metal-enriched fluids which were trapped at depth and overpressured. These fluids contained high concentrations of gold, arsenic, iron, and sulfur.

2. During a period of uplift early in this orogeny, fault propagation resulted in the tapping of these fluids and allowed their escape to a level in the crust corresponding to the Ordovician-Silurian contact. Here, they selectively penetrated and pyritized suitable lithological units adjacent to the fissures (dominantly the banded black shale lithology underlying banded black shale-siltstone or shale-siltstone units). During deformation, the more competent siltstones controlled the style of fold, whereas the less competent shales deformed disharmonically with much bedding plane slip and dilatancy. Migrating fluids thus moved laterally into the shales and introduced pyrite into the fractures and bedding plane dilatancies and

also caused pyritization of individual shale beds. Little quartz or carbonate was introduced at this time, though some fractures, perhaps opened by fluid pressures, were filled with coarsely crystalline pyrite, quartz, and carbonate. Increasing amounts of arsenopyrite were introduced at a later stage as euhedral porphyroblasts incorporating grains and framboids of earlier pyrite.

3. The development of upright cylindrical folds and associated cleavage as orogenesis reached its peak, led to the deformation of pyritic horizons and their associated veinlets. Ptygmatic veins, bound-naged pyrite bands, pull-apart structures, pressure shadows, and cleavage deflection through veins were produced at this time. Early sulfides and gangue minerals were recrystallized or ruptured and were reemplaced with later quartz and carbonate which also penetrated dilations produced in pressure shadows adjacent to sulfide grains.

4. Continued deformation led to the formation of tight asymmetric folds and reverse faults (with dips  $> 70^\circ$ ). Some faults were minor and directly related to the folds whereas others transgressed these folds. Such faults may have deflected along weaker, pyritized, horizons on anticlinal fold limbs (the Roman lode fissure?; see Fig. 9) before crossing the axial plane of the adjacent synclinal fold and steepening once again. Shear couples acting on these faults resulted in the creation of locally concordant dilational openings around the crests of anticlinal folds, tensional shear fissures in the footwall of the fault, and shear zones associated with the main fault into which siliceous fluids could be introduced.

5. The emplacement of the main auriferous quartz veins from fluids at temperatures between  $345^\circ$  and  $450^\circ\text{C}$  took place in rocks whose ambient temperatures were probably between  $300^\circ$  and  $350^\circ\text{C}$ . Locally, these veins had a saddle reef structure whereas elsewhere they formed sheeted vein systems in shear zones (Long adit) or wedge-shaped planar veins in tensional fissures (Mitchell adit). These extensional fissures are probably equivalent to the "step and side veins" described by Haynes (1986) for turbidite-hosted gold deposits in eastern Nova Scotia. Variations in the attitude of the shear zone resulted in either flat-lying podiform veins or steeply inclined sheeted veins with irregular quartz bosses. Additional sulfidation of the country rock took place adjacent to many of these veins.

6. Late-stage, high-angle, reverse faulting further disrupted the folded strata at Dolaucothi and caused rupture of many of the veins, especially the flat-lying reefs. It was probably at this time that lower temperature, late-stage, hydrothermal fluids invaded these fractures, introducing both hydromuscovite and cookeite, along with minor amounts of quartz and carbonate.

7. A period of normal faulting under a post-Caledonide tensional regime then followed, resulting in the Clochdy Gwenno and Lead Lode faults. Base metal sulfides were introduced into these faults during the metalliferous event which formed the central Wales lead-zinc mining field (355–359 Ma). Sphalerite-cemented hydraulic breccias, intersected in drill holes, are probably also related to this ore-forming phase. Remobilization of gold probably took place during this thermal event, along with the introduction of copper, lead, and zinc sulfides into the main-stage quartz veins so that microfractures were filled with an intimately intergrown mixture of these minerals.

### Acknowledgments

Much of the work described in this paper was undertaken with research funding provided by Anglo-Canadian Exploration Ltd. of Toronto and by donations toward the cost of diamond drilling provided largely by BP Minerals Ltd., Ryan International Ltd., Consolidated Goldfields Ltd., Zambia Consolidated Copper Mines Ltd., Aber Resources Ltd. of Vancouver, Riofinex Ltd., and by smaller donations from various organizations and ex-graduates of University College, Cardiff. All of this assistance is gratefully acknowledged, as is the technical assistance rendered by G. Williams of Quest Exploration Ltd. The authors are particularly indebted to *Economic Geology* reviewers, who made invaluable comments on the text, and to P. C. Fisher of the Geology Department, University of Wales, Cardiff, for XRF and XRD analyses.

### REFERENCES

- Al-Atia, M. J., and Barnes, J. W., 1974, Rubidium: A primary dispersion pathfinder at Ogofau gold mine, southern Wales, in Elliot, I. L., and Fletcher, W. K., eds., *Geochemical exploration 1974*; Amsterdam, Elsevier, p. 341–352.
- Annels, A. E., and Burnham, B. C., 1986, *The Dolaucothi gold mines; geology and mining history*; Cardiff, Univ. College, p. 62.
- Annels, A. E., and Hellewell, E. G., 1988, The orientation of bedding, veins and joints in core; a new method and case history: *Internat. Jour. Mining Geol. Eng.*, v. 5, p. 307–320.
- Bergstrom, S. M., 1980, Conodonts as palaeotemperature tools in Ordovician rocks of the Caledonides and adjacent areas in Scandinavia and the British Isles: *Geol. Foren. Stockholm Forh.*: v. 102, p. 377–392.
- Bevins, R. E., and Rowbotham, G., 1983, Low-grade metamorphism within the Welsh sector of the paratectonic Caledonides: *Jour. Geology*, v. 18, p. 131–167.
- Bevins, R. E., Robinson, D., Rowbotham, G., and Dunkerley, P. N., 1981, Low-grade metamorphism in the Welsh Caledonides: Conference report: *Geol. Soc. London Jour.*, v. 138, p. 634.
- Boyle, R. W., 1979, The geochemistry of gold and its deposits: *Canada Geol. Survey Bull.* 280, p. 584.
- 1986, Gold deposits in turbidite sequences: Their geology, geochemistry, and history of the theories of their origin: *Geol. Assoc. Canada Spec. Paper* 32, p. 1–14.
- Brammall, A., Leech, J. G. C., and Bannister, F. A., 1937, The paragenesis of cookeite and hydromuscovite associated with gold

- at Ogofau, Carmarthenshire; *Mineralog. Mag.* v. 24, p. 506–520.
- Davies, K. A., 1933, The geology of the country between Aber-gwesyn (Breconshire) and Pumpsaint (Carmarthenshire): *Geol. Soc. London Quart. Jour.* v. 89, p. 172–201.
- Dewey, J. F., 1982, Plate tectonics and the evolution of the British Isles: *Geol. Soc. London Jour.*, v. 139, p. 317–412.
- Friedman, I., and O'Neil, J. R., 1977, Compilation of stable isotope fractionation factors of geochemical interest: U. S. Geol. Survey Prof. Paper 440-KK, p. KK1–KK12.
- Fyfe, W. S., and Henley, R. W., 1973, Some thoughts on chemical transport processes, with particular reference to gold: *Minerals Sci. Eng.*, v. 5, p. 295–303.
- Gale, N. H., Beckinsale, R. D., and Wadge, A. J., 1980, Discussion of a paper by McKerrow, Lambert and Chamberlain on the Ordovician, Silurian and Devonian timescales: *Earth Planet. Sci. Letters*, v. 51, p. 9–17.
- Goldfarb, R. J., Leach, D. L., Miller, M. L., and Pickthorn, W. J., 1986, Geology, metamorphic setting and genetic constraints of epigenetic lode-gold mineralization within the Cretaceous Valdez Group, south-central Alaska: *Geol. Assoc. Canada Spec. Paper 32*, p. 87–106.
- Groves, D. I., Golding, S. D., Rock, N. M. S., Barley, M. E., and McNaughton, N. J., 1988, Archaean carbonate reservoirs and their relevance to the fluid source for gold deposits: *Nature*, v. 331, p. 254–257.
- Hall, G. W., 1971, Metal mines of southern Wales: Gloucester, Jennings, p. 39–48.
- Haynes, S. J., 1986, Geology and chemistry of turbidite-hosted gold deposits, greenschist facies, eastern Nova Scotia: *Geol. Assoc. Canada Spec. Paper 32*, p. 161–178.
- Henley, R. W., 1973, Solubility of gold in hydrothermal chloride solutions: *Chem. Geology*, v. 11, p. 73–87.
- Holman, B. W., 1911, Gold deposits of Cothy, South Wales: *Mining Mag.*, v. 4, p. 374–378.
- Ineson, P. R., and Mitchell, J. G., 1975, K-Ar isotopic age determinations from some Welsh mineral localities: *Inst. Mining Metallurgy Trans.*, v. 84, sec. B, p. 7–16.
- James, D. M. D., and James, J., 1969, The influence of deep fractures on some areas of Ashgillian-Llandoveryian sedimentation in Wales: *Geol. Mag.*, v. 106, p. 562–582.
- Jones, O. T., 1912, The geological structure of central Wales and the adjoining regions: *Geol. Soc. London Quart. Jour.*, v. 68, p. 326–344.
- Keppie, J. D., Boyle, R. W., and Haynes, S. J., 1986, Turbidite-hosted gold deposits: *Geol. Assoc. Canada Spec. Paper 32*, 186 p.
- Kokelaar, B. P., Howells, M. F., Bevins, R. E., Roach, R. A., and Dunkerley, P. N., 1984, The Ordovician marginal basin of Wales: *Geol. Soc. London Spec. Pub.* 16, p. 245–269.
- Kubler, B., 1967, La cristallinité de l'illite et les zones tout a fait supérieures du métamorphisme: Etages Tectonique Colloquium, à la Baconnière, Univ. Neuchâtel, Suisse, April 18–21, 1966, p. 105–121.
- Liou, J. G., Maruyama, S., and Cho, M., 1985, Phase equilibria and mineral parageneses of metabasites in low-grade metamorphism: *Mineralog. Mag.*, v. 49, p. 321–333.
- McKerrow, W. S., Lambert, R. St. J., and Chamberlain, V. E., 1980, The Ordovician, Silurian and Devonian timescales: *Earth Planet. Sci. Letters*, v. 51, p. 1–8.
- Mueller, R. F., and Saxena, S. K., 1971, *Chemical petrology*: New York, Springer-Verlag, 394 p.
- Nagelschmidt, Z., 1937, in *Mineral powder diffraction file, data book*: Internat. Centre Diffraction Data, Pennsylvania, 1980, Pub. JCPDS, p. 453.
- Nelson, T. R. H., 1944, Gold mining in south Wales: *Mine Quarry Eng.*, v. 9, p. 3–10, p. 33–38, p. 55–60.
- Olson, R. A., 1984, Genesis of palaeokarst and strata-bound zinc-lead sulfide deposits in a Proterozoic dolostone, northern Baffin Island, Canada: *ECON. GEOL.*, v. 79, p. 1056–1103.
- Paterson, C. J., 1986, Controls on gold and tungsten mineralization in metamorphic-hydrothermal systems, Otago, New Zealand: *Geol. Assoc. Canada Spec. Paper 32*, p. 25–40.
- Phillips, W. E. A., Stillman, C. J., and Murphy, T., 1976, A Caledonian plate tectonic model: *Geol. Soc. London Jour.*, v. 132, p. 579–609.
- Potter, R. W., 1977, Pressure corrections for fluid inclusion homogenization temperatures based on the volumetric properties of the system NaCl-H<sub>2</sub>O: *U.S. Geol. Survey Jour. Research*, v. 5, p. 603–607.
- Robinson, D., and Bevins, R. E., 1986, Incipient metamorphism in the lower Palaeozoic marginal basin of Wales: *Jour. Metamorphic Geology*, v. 4, p. 101–113.
- Robinson, D., Nicholls, R. A., and Thomas, L. J., 1980, Clay mineral evidence for low-grade Caledonian and Variscan metamorphisms in south-western Dyfed, south Wales: *Mineralog. Mag.*, v. 43, p. 857–863.
- Steed, G. M., Annel, A. E., Shrestha, P. L., and Tater, P. S., 1976, Geochemical and biogeochemical prospecting in the area of the Ogofau gold mines, Dyfed, Wales: *Inst. Mining Metallurgy Trans.* v. 85, sec. B, p. 109–117.
- Tater, P. S., 1975, The Ogofau gold bearing lodes: Their structural control and primary geochemistry: Unpub. M.Sc. thesis, Univ. Wales, 177 p.
- Taylor, H. P., Jr., 1979, Oxygen and hydrogen isotope relationships in hydrothermal mineral deposits, in Barnes, H. L., ed., *Geochemistry of hydrothermal ore deposits*: New York, Wiley Intersci., p. 236–277.